BNL-64945-98/10-Rev.

MODEL CORRELATIONS FOR OZONE, REACTIVE NITROGEN AND PEROXIDES FOR NASHVILLE IN COMPARISON WITH MEASUREMENTS: IMPLICATIONS FOR O_3-NO_x-HYDROCARBON CHEMISTRY

S. Sillman, D. He, and M. R. Pippin
Department of Atmospheric, Oceanic
and Space Sciences
University of Michigan
Ann Arbor, MI 48109-2143

P. H. Daum, D. G. Imre, L. I. Kleinman,
J. H. Lee, and J. Weinstein-Lloyd
Environmental Chemistry Division
Department of Applied Science
Brookhaven National Laboratory
Upton, NY 11973-5000

Original Manuscript Date: November 1997

Publisahed in
Journal of Geophysical Research

By acceptance of this article, the publisher and/or recipient acknowledges the U.S. Government's right to retain a nonexclusive, royalty-free license in and to any copyright covering this paper.

Research by BNL investigators was performed under the auspices of the U.S. Department of Energy under Contract No. DE-AC02-98CH10886.

Model correlations for ozone, reactive nitrogen, and peroxides for Nashville in comparison with measurements: Implications for O_3-NO_x-hydrocarbon chemistry

Sanford Sillman, Dongyang He, and Margaret R. Pippin

Department of Atmospheric, Oceanic, and Space Sciences, University of Michigan, Ann Arbor

Peter H. Daum, Daniel G. Imre, Lawrence I. Kleinman, and Jai Hoon Lee

Environmental Chemistry Division, Brookhaven National Laboratories, Upton, New York

Judith Weinstein-Lloyd

Chemistry/Physics Department, State University of New York, Old Westbury

Abstract. We present an analysis of correlations between O_3, NO_x reaction products (NO_z), and peroxides in photochemical models for polluted environments in comparison with measurements in the vicinity of Nashville, Tennessee. This analysis is associated with the use of O_3/NO_z, H_2O_2/NO_z, and similar ratios as indicators for the relative impact of NO_x and hydrocarbons (volatile organic compounds, VOC) on ozone formation. The measurements are used both to evaluate the NO_x-VOC indicator theory and to identify NO_x-VOC chemistry in Nashville. Results show that a linear correlation exists between O_3 and the sum $2H_2O_2+NO_z$, consistent between models and measurements. The ratio $O_3/2H_2O_2+NO_z$ has a near-constant value in both the Nashville urban plume and surrounding rural area. A similar correlation is found with total peroxides (O_3 versus 2peroxides+NO_z) but with greater scatter. The correlations between O_3, NO_z, and peroxides are consistent with an assumed dry deposition rate of 5 cm s^{-1} for H_2O_2 and HNO_3. Changes in dry deposition and RO_2 reaction rates cause minor adjustments in the NO_x-VOC-indicator analysis for H_2O_2/NO_z. Measured indicator ratios for Nashville are close to the NO_x-VOC transition predicted by models and form an intermediate point between previous measurements for Atlanta (NO_x sensitive) and Los Angeles (VOC sensitive). The model ozone production efficiency ($P(O_3)/L(NO_x)$) is 3-4, significantly lower than would be derived from the O_3-NO_z slope (5-8).

1. Introduction

A great deal of information about the chemistry of ozone production can be derived from correlations between ozone, reactive nitrogen, and peroxides. Correlations between ozone and total reactive nitrogen (NO_y) and between ozone and NO_x reaction products (NO_z) have been used extensively, both as a basis for evaluating the performance of photochemical models and for determining the ozone production efficiency, that is, the rate of ozone production per loss of NO_x ($P(O_3)/L(NO_x)$) [*Liu et al.*, 1987; *Lin et al.*, 1988; *Trainer et al.*, 1993; *Olszyna et al.*, 1994; *Kleinman et al.*, 1994]. More recently, *Sillman* [1995] proposed that a linear correlation should be observed between ozone and the sum of $2H_2O_2+NO_z$, reflecting the balance between sources and sinks of odd hydrogen radicals. Sillman also found that ratios involving ozone, NO_z and peroxides can be used as "indicators" for the chemistry of ozone, NO_x, and volatile organic compounds (VOC); in that low values of indicator ratios correspond to VOC-sensitive ozone chemistry, while high values correspond to NO_x-sensitive chemistry. Thus measured NO_z and peroxides can be used to evaluate several aspects of ozone chemistry in polluted environments. Reactive nitrogen and peroxides exported from polluted regions also have a significant impact on the chemistry of the remote troposphere [e.g., *Singh et al.*, 1992].

The recent Middle Tennessee Ozone Study provides a unique opportunity to evaluate theoretical results associated with these species. The study included extensive measurement of reactive nitrogen, H_2O_2, and organic peroxides in aircraft flights that included both the Nashville urban plume and the surrounding rural area. These measurements can be used both to examine species cross correlations in comparison with photochemical models and to examine the validity of these species as NO_x-VOC indicators.

This paper presents results of a combined urban and regional-scale Eulerian photochemical model for Nashville in combination with measured O_3, NO_z, and peroxides from aircraft flights. Model results are presented for the convective mixed layer near Nashville during the afternoon of July 11, July 13, and July 18. Comparisons are shown with measurements from the G1 aircraft flights (described by *Hubler et al.* [this issue]). Similar measurements were also made by R. Valente and R. L. Tanner (Tennessee Valley Authority (TVA), described by *Hubler et al.*) but have not been included in the current study. Model results include updated chemistry and sensitivity to changes in chemistry and dry deposition rates. The current evaluation addresses four broad topics as follows: (1) use of model correlations between O_3, NO_z, and peroxides in comparison with measurements as a basis for evaluating model assumptions, especially with regard to deposition rates, (2) use of measurements to evaluate the theory from *Sillman* [1995] and *Sillman et al.* [1997] that O_3/NO_z and H_2O_2/NO_z can be used as indicators for O_3-NO_x-VOC chemistry, (3) use of measured indicator ratios and models to evaluate O_3-NO_x-VOC chemistry for Nashville, and (4) impact of removal processes on the correlation between O_3 and NO_z and its implication for ozone production efficiency.

Results show a linear correlation between O_3 and the sum $2H_2O_2+NO_z$ and between O_3 and the sum 2peroxides+NO_z, which is largely consistent between models and measurements.

Results of model-measurement comparisons are also generally consistent with the interpretation of NO_z and peroxides as NO_x-VOC indicators. However, the recent changes in peroxide chemistry and dry deposition rates in models have caused a downward shift in the NO_x-VOC transition for indicator ratios that involve peroxides. Measurements are consistent with these updated indicator transition values. Model results and measurements for Nashville both suggest that ozone production is close to the transition between NO_x-sensitive and VOC-sensitive chemistry. The Nashville measurements contrast with previous measurements in Atlanta (suggesting NO_x-sensitive chemistry) and Los Angeles (suggesting VOC-sensitive chemistry) [*Sillman*, 1995; *Sillman et al.*, 1997]. Model results also suggest that the ozone production efficiency is 40-50% lower than the measured slope between O_3 and NO_z.

2. Simulation Methods

The simulations are based on the Michigan modeling system [*Sillman et al.*, 1993] with various modifications. This system consists of a coarse-resolution regional-scale model [*Sillman et al.*, 1990a], used to represent photochemistry over the eastern half of the United States, combined with an fine-resolution model that represents photochemistry of a 180x180 km region around Nashville (see Figure 1). The coarse-resolution model has 400x480 km horizontal resolution in combination with a subgrid structure that separately represents the chemistry of rural areas, urban plumes and power plant plumes. Previous results [*Sillman et al.*, 1990a, b] have shown that this model is able to represent region-wide average chemistry, especially in situations that involve long-range transport of ozone. This model has also been used as a component in Eulerian models for the global troposphere [*Jacob et al.*, 1993]. The coarse-grid regional model is used to provide boundary conditions to the urban model for Nashville (one-way nesting). The urban model has 5x5 km horizontal resolution.

Both models use three vertical levels to represent photochemistry and transport in the polluted lower troposphere: a lower level that represents the convective mixed layer, a second level that represents nighttime air that becomes entrained in the daytime convective mixed layer, and a level that represents tropospheric air immediately above the top of the daytime convective mixed layer. The height of the first level changes with time of day, reflecting the evolution of the convective mixed layer, with entrainment from above, during the daytime and the formation of a new stable layer (with height 100 m) as the boundary layer stabilizes at night. A new entrainment layer (second level) is also formed as the boundary layer stabilizes at night, with height equal to the mixing height from the previous day. During the next day this entrainment layer becomes largely incorporated in the convective mixed layer (first level), and the remainder (if the mixing height during the next day is lower than the height of the entrainment layer) becomes incorporated in the third level of model. The third level provides a reservoir that represents injection of pollutants above the daytime mixed layer (when the mixed layer height has decreased from one day to the next) and reentrainment into the mixed layer (when the mixed layer height has increased from one day to the next). The model vertical structure also includes modifications that reflect the impact of suppressed vertical mixing over large bodies of water [*Sillman et al.*, 1993], although this has no impact on Nashville. The heights of each level is also allowed to vary horizontally, reflecting differences in mixing heights in different locations. Layer heights are advected horizontally as described by *Sillman et al.* [1993].

The current version of the model does not include representation of near-surface processes (0-50 m) and does not include a separate representation of large point source plumes in the fine-grid domain. A surface level would be needed to insure accurate representation of primary species, especially isoprene, which show strong variation with height even during periods of rapid convective mixing [*Andronache et al.*, 1994; *Sillman et al.*, 1995]. The current version represents average concentrations in the daytime mixed layer only, not surface concentrations. Subgrid representation of large point sources was found to have an impact on model photochemistry within 50 km of the emission source [*Kumar and Russell*, 1996].

Other assumptions include horizontal advection based on second-order moments [*Prather*, 1986] for the coarse-resolution component and on *Smolarkiewicz* [1983] for the urban model. Photolysis rates are based on *Madronich* [1987]. An aerosol optical depth of 0.68 was assumed, representing moderately polluted conditions typical of the eastern United States [*Flowers et al.*, 1969]. The photolysis rate calculation assumes clear skies, a total O_3 column of 325 Dobson units (DU), surface albedo of 0.15, and single-scattering albedo of 0.75. Concentrations at the upwind boundary of the regional model are representative of remote continental locations: 40 ppb O_3; 0.15 ppb NO_x; 0.1 ppb PAN; 1 ppb H_2O_2; 200 ppb CO; 1700 ppb CH_4; and 4 ppbC volatile organics. The model was exercised for July 10-13 and July 16-18, 1995.

Chemistry, dry deposition, meteorological input and emissions are all subjects of special investigation in this study and are described in detail here.

2.1. Chemistry

The model uses a photochemical mechanism based on *Lurmann et al.* [1986] with numerous updates, including updated reaction rates [*DeMore et al*., 1994], RO_2+HO_2 reactions [*Jacob and Wofsy*, 1988] and chemistry of isoprene and related species based on *Paulson and Seinfeld* [1992]. The model also includes updated RO_2-HO_2 reaction rates and additional RO_2-RO_2 reactions recommended by *Kirchner and Stockwell* [1996]. The reaction rates for organic peroxides with OH were updated based on recommendations from *Stockwell et al.* [1997], which are lower than the values used by Paulson and Seinfeld for peroxides derived from isoprene. Some minor modifications and extensions were made to the chemistry of organic (RO_2) radicals, especially in association with isoprene. We assume that all RCO_3 radicals that form PAN-like organic nitrates (e.g., $CH_3CH_2CCO_3$, which forms peroxy methacrylic nitric anhydride, or MPAN) undergo a self-reaction with the same rate as CH_3CO_3, and also react with CH_3CO_3 and CH_3O_2. These RCO_3 reactions are assumed to produce the same intermediate hydrocarbons as are produced in the equivalent RCO_3-NO reactions, by analogy to Kirchner and Stockwell. The RO_2 radicals associated with methylvinylketone, methacrolein, and other isoprene reaction products are each

assumed to react with HO_2 to form an organic peroxide, with the same reaction rates and properties of the organic peroxide associated with isoprene RO_2 radicals in the work of *Stockwell et al.* [1997]. A separate calculation is also made with RO_2-HO_2 and RO_2-RO_2 rate constants equal to the "old values" shown by Kirchner and Stockwell. These older rate estimates are similar to the values used in the original analysis of peroxides and photochemical indicators by *Sillman* [1995].

2.2. Dry Deposition

Previously, *Sillman et al.* [1990a, 1995] used dry deposition estimates of 1 cm s^{-1} for H_2O_2 and 2.5 cm s^{-1} for HNO_3. More recently, *Hall and Claiborn* [1997] reported higher (5 cm s^{-1}) deposition rates for H_2O_2 from flux measurements in Canada. Their results also suggested that dry deposition of H_2O_2 is limited only by atmospheric dynamics and should therefore be equal to the deposition rate of HNO_3. Dry deposition during the Nashville event is expected to be lower than measured by Hall and Claiborn in Canada because winds were unusually light. Following a recommendation from Hall (private communication, 1997) we have used a dry deposition velocity of 2.5 cm s^{-1} for both H_2O_2 and HNO_3 in our standard model scenario. However, deposition is recognized as a major source of uncertainty in model calculations for both peroxides and NO_z. Alternative scenarios have dry deposition of 5 cm s^{-1} for both H_2O_2 and HNO_3, corresponding to Hall and Claiborn, 1997, and 1 cm s^{-1} for H_2O_2 and 2.5 cm s^{-1} for HNO_3, corresponding to the previous NO_x-VOC indicator analysis in Sillman (1995a). Dry deposition of organic peroxides is 0.8 cm s^{-1}, also based on Hall and Claiborn (1997). Other deposition velocities are: O_3 and NO_2, 0.6 cm s^{-1}; NO, 0.1 cm s^{-1}; and PAN, 0.25 cm s^{-1}. Wet deposition is not included.

2.3. Meteorology

Wind fields and temperature profiles were derived from the Rapid Update Cycle (RUC) model, a dynamic model, a prognostic model developed by *Benjamin et al.* [1994]. This is a mesoscale analysis/forecast system that operates on a 3-hour cycle to provide high-frequency updates of tropospheric conditions and short-range forecasts over the lower 48 United States and adjacent areas. The height of the convective mixed layer is derived by using measured temperature gradients to identify the critical inversion heights [*Heffter*, 1980; see also *Marsik et al.*, 1995]. Like most prognostic models for this spatial scale, the RUC is driven by a relatively sparse network of measurement sites operated by the National Weather Service. These estimates are especially problematic during periods of light and variable winds, which were typical of the episode in Nashville on July 11-13. In the standard model scenario, winds for the urban subsection were derived from measured wind and temperature profiles at New Hendersonville (see description by *Meagher et al.* [this issue] and *McNider et al.* [this issue]). An additional model scenario was tested in which wind fields, temperatures and mixing heights from the RUC were used in both the urban and regional model components, replacing the measured values from New Hendersonville in the Nashville urban domain. The RUC results have higher wind speeds and significantly higher afternoon mixing heights in comparison with the values derived from measurements at New Hendersonville (RUC equal to 2800 m, New Hendersonville equal to 2100 m).

2.4. Emissions

Biogenic emissions are derived from the BEIS2 inventory [*Geron et al*., 1994] with 20x20 km resolution. Anthropogenic emissions for the regional model component were derived from the NAPAP 1990 inventory [*Environmental Protection Agency* (EPA), 1993] for summer weekdays, which is available with 20x20 km resolution. For the Nashville urban domain we used an inventory developed as part of the 1988 State Implementation Plan (SIP) for Nashville, developed by W. Davis (University of Tennessee, Knoxville) and used with permission from J. Walton (Tennessee Department of Environmental Quality). This inventory was prepared with 5x5 km resolution based on conditions for June 23-24, 1988, a period that was meteorologically similar to the 1995 event, based on the NAPAP 1985 inventory.

2.5. Alternative Scenarios

Scenarios were selected that would examine the impact of major model uncertainties, with emphasis on factors (e.g., deposition) that were likely to have a large impact on reactive nitrogen and peroxides, and their interpretation of indicators for NO_x-VOC chemistry. In addition, scenarios were designed with changed emission rates that would change the predicted response to reduced NO_x and VOC. The latter scenarios were included in order to test the robustness of model NO_x-VOC predictions and to explore the use of indicator ratios as evaluators of scenarios with different NO_x-VOC chemistry. The scenarios, along with abbreviations used in plots and tables, are as follows: J13, etc.: standard scenario (where J11, J12, J13, and J18 indicate the date in July, 1995); D1: dry deposition of H_2O_2 reduced to 1 cm s^{-1}, equivalent to the value used by *Sillman* [1995]; D5: dry deposition of H_2O_2 and HNO_3 increased to 5 cm s^{-1}; J13B, D1B, and D5B: biogenic emissions reduced by 75%, approximately equal to the emission estimates from the older BEIS1 inventory (see discussion by *Geron et al.* [1994]); Ch: older chemical rate constants for RO_2-HO_2 and RO_2-RO_2 reactions, discussed above; HC: emissions of anthropogenic and biogenic hydrocarbons increased by 50% relative to the standard scenario, reflecting uncertainties in emission rates [e.g., see *Geron et al.*, 1994; *Fujita et al*., 1992]; D5H: dry deposition of H_2O_2 and HNO_3 increased to 5 cm s^{-1}; emission of anthropogenic (but not biogenic) hydrocarbons increased by 50% relative to the standard scenario; RUC: wind fields and mixing heights for the Nashville urban model derived from the RUC rather than from the New Hendersonville measurements. This results in a mixing height of 2900 m during the afternoon of July 13, in contrast with 2100 m in the standard scenario; RUCH: RUC mixing heights and emissions of anthropogenic hydrocarbons increased by 50%; RH: relative humidity reduced by 50% (included as a test of chemistry rather than as a realistic representation of the Nashville event); and T: temperature reduced by 10 K (included as a test of chemistry rather than as a realistic representation of the Nashville event). Sensitivity to NO_x. and VOC is tested for each model scenario by repeating the simulation with a 35% reduction (relative to the

initial scenario, applied to both the urban and regional model domains) in either anthropogenic VOC or NO_x.

3. Meteorology

Meteorology during the Nashville event and the extent of measurements are described elsewhere [*Meagher et al.*, this issue; *McNider et al*., this issue]. A brief summary is presented here. The simulated events, July 11-13 and July 18, were characterized by generally high sunlight and warm temperatures (30°-35°C during the daytime). July 11-13 also had unusually light winds (<2 m s^{-1}), while July 18 had stronger winds (5 m s^{-1}). Both the RUC prognostic model and the measurements at New Hendersonville reported extremely light winds (<1 m s^{-1}) on July 13 and stronger winds (1-2 m s^{-1}) on July 11 and 12. The model results reflect this difference. In addition, the model wind fields for July 12 result in a partial overlap of the Gallatin power plant plume and the Nashville urban plume. The Gallatin plant is located 35 km NE of Nashville, upwind on July 12 (see Figure 1).

4. Measurement Techniques

Measurements are from the Department of Energy (DOE) G-1 aircraft flights (described by *Meagher et al.* [this issue]). The G-1 was equipped with a suite of instrumentation to measure the chemical species of interest. Oxides of nitrogen (NO, NO_x, and NO_y) were determined using a three-channel detector [*Daum et al.*, 1996; *Kleinman et al.*, 1994] in which the instrument measures NO directly by O_3 chemiluminescence, NO_2 by conversion to NO with UV-photolysis, and, NO_y by reduction to NO on a hot (350° C) molybdenum catalyst. The uncertainty in measurement of the NO concentration for 10 s averaged data is estimated to be 20 pptv + 15% of the NO concentration, 20 pptv + 15% of the NO_2 concentration, and 50 pptv + 15% of the NO_y concentration. Ozone was measured using a commercial UV absorption detector (Thermo Environmental Instruments, Model 49-100). The estimated uncertainty in measurement of the O_3 concentration is 5 ppbv. Instrument uncertainty for 1 min averaged date is estimated to be 30 ppbv + 15% of the measured concentration.

Peroxides were determined with a three-channel continuous flow analyzer using a different chemistry in each channel to speciate H_2O_2, methylhydroperoxide (MHP, CH_3OOH), and hydroxymethyl hydroperoxide (HMHP, $HOCH_2OOH$) [*Lee et al.*, 1990, 1994; *Weinstein-Lloyd et al*., this issue]. The instrument was calibrated daily using aqueous-phase standards prepared from 3% peroxide stock solution that had been titrated against standardized potassium permanganate. Air and liquid flow rates were determined several times during the program. The uncertainty associated with converting aqueous standards to gas-phase concentration is approximately 15%; derived values of individual peroxide concentrations, which include a 12% uncertainty in the Henry's law constant for MHP, may be as high as 25%. The 10 to 90% response time of the instrument was 110 s.

Measurements were made along a perimeter around Nashville approximately 25 km from the Nashville city center (see Figure 1) at altitudes 1150, 750, and 450 m between 1300 and 1400 local standard time (LST). These are described in greater detail elsewhere [see *Meagher et al.*, this issue; *Hubler et al.*, this issue; *Weinstein-Lloyd et al.*, this issue].

5. Results: Correlation Between O_3, NO_z, and Peroxides

Simulated O_3 throughout the fine-resolution model domain at 1400 LT, July 13 is shown in Figure 1, along with the flight path. The region of high O_3 associated with Nashville, and low O_3 in the vicinity of the Gallatin and Cumberland power plants, are both visible in the figure. Peak O_3 in the model occurs just 5 km west of the Nashville urban center, reflecting the very low wind speeds on this day. Peak O_3 along the aircraft transects was found along the perimeter 25 km north of the urban center. The subsequent model results (for species cross correlations, etc.) are all reported for the region interior to the flight path perimeter shown in Figure 1, including all locations within 25 km of downtown Nashville.

The correlation between O_3, NO_z, and peroxides is illustrated in Figure 2 (from measurements) and Figure 3 (from the standard model scenario). Reference lines are shown in both figures for a slope of 9 and y-intercept of 40 ppb (approximately equal to the correlation between O_3 and NO_z in previous measurements at rural sites by *Trainer et al.* [1993]) and for a constant ratio of 7. These lines are shown to facilitate comparison between measurements and model scenarios and do not represent fits to data. Linear least squares coefficients associated with the figures are summarized in Table 1.

Results from the model and measurements both show a positive correlation between O_3 and NO_z, between O_3 and the sum $2H_2O_2+NO_z$, and between O_3 and the sum $2(H_2O_2+ROOH)+NO_z$, where ROOH represents organic peroxides. Although there is a good qualitative agreement between the model and measured correlations, there are also significant discrepancies. A detailed description follows.

5.1. O_3 Versus NO_z

The correlation between O_3 and NO_z in rural locations has been extensively discussed [*Trainer et al*., 1993; *Olszyna et al.*, 1994; *Kleinman et al.*, 1994; *Daum et al.*, 1996]. The results for Nashville show that O_3 increases with NO_z in a manner similar to the previous rural measurements. However, there are two important differences between the model results and measurements. First, the model tends to predict higher NO_z for a given O_3 throughout the domain (e.g., at O_3=90 ppb, NO_z=7-12 ppb in the model, 5-6 ppb measured). Second, there is a shift toward lower O_3 relative to NO_z at the center of Nashville (e.g., O_3=120 ppb, NO_z=20 ppb; versus O_3=120 ppb, NO_z=15 ppb farther downwind). There is no equivalent shift in measured O_3 relative to NO_z, possibly because the aircraft measurements did not include the center of Nashville. The slope between O_3 and NO_z (defined by least squares coefficient a_1 for $O_3 = a_0+a_1NO_z$) is also lower in the model than in measurements (4.0 modeled; 5.7 measured; see Table 1). The modeled and measured slopes are both lower than in previous rural measurements (8.5 by *Trainer et al.* [1993]; 12 by *Olszyna et al.* [1994]). The value of the ratio O_3/NO_z (a value distinct from the slope) is also lower in the model than in measurements (see Figures 4 and 5).

This model-measurement discrepancy might be interpreted in two ways. The model underprediction of the ratio O_3/NO_z, especially in association with peak O_3 (7 modeled, 9 measured, see Table 2) might be interpreted as evidence for erroneous NO_x-VOC sensitivity in the model, as in the works of *Sillman et al.* [1995], and *Sillman* [1995]. Alternatively, it might be hypothesized that the model has underestimated removal rates for reactive nitrogen, especially through dry deposition of HNO_3. Both possibilities are investigated in alternative model scenarios, discussed below.

In contrast with some previous measurements, the O_3-NO_z slope shows little tendency to decrease with increasing NO_z. There is a statistically significant decrease in the O_3-NO_z slope between low and high O_3 (measured slope equal to 6.1 for O_3<110 ppb, 4.8 for O_3>110 ppb), but this is a much smaller decrease than reported for other measurements [e.g., *Daum et al.*, 1996]. However the ratio O_3/NO_z shows a large decrease between rural locations with relatively low O_3 (measured O_3/NO_z= 15-25 at O_3=80 ppb) and locations associated with peak O_3 in the Nashville plume (measured O_3/NO_z= 9 measured, at peak O_3). This change in the O_3/NO_z ratio between rural and urban locations is illustrated more clearly in Figure 4. A similar decrease in O_3/NO_z between photochemically aged rural locations and the urban peak O_3 was found in measurements by *Daum et al.* [1996]. As will be discussed below, this decrease in the O_3/NO_z ratio is associated with the difference in NO_x-VOC chemistry between rural and urban locations. Model results (Figure 5) also show a decrease in O_3/NO_z between rural and urban locations (O_3/NO_z=7−14 at O_3=80 ppb, 7 at peak O_3). However, the change between rural and urban locations is less consistent in the model than in measurements and there are some rural locations in the model with O_3/NO_z as low as in the urban center. These rural locations with low O_3/NO_z (modeled but not measured) might represent air in which NO_z was produced primarily at nighttime, without concurrent production of O_3.

5.2. O_3 Versus $2H_2O_2+NO_z$

A strong linear correlation between O_3 and the sum $2H_2O_2+NO_z$ appears in both measurements (Figure 2) and the model (Figure 3). There is excellent agreement between model and measurements, although the model shows a slight tendency to overestimate the sum $2H_2O_2+NO_z$ (e.g., maximum $2H_2O_2+NO_z$ in the model equal to 25, measured maximum equal to 21). In contrast with results for O_3 versus NO_z, the ratio $O_3/(2H_2O_2+NO_z)$ shows little variation between rural locations ($O_3/2H_2O_2+NO_z$=7-8 at O_3=80 ppb) and the urban ozone peak ($O_3/2H_2O_2+NO_z$=7 at O_3=140 ppb). This lack of variation in the ratio $O_3/2H_2O_2+NO_z$ is also shown in Figures 4 and 5. The measured ratio is slightly higher than the model values ($O_3/2H_2O_2+NO_z$=6.5 at O3=80 ppb, $O_3/2H_2O_2+NO_z$=5.6 at O_3=135 ppb). Similar results were reported in models by *Sillman* [1995] and in measurements by *Daum et al.* [1996], although *Staffelbach et al.* [1997a, b] measured higher ratios and greater variability between the urban plume and surrounding rural area.

Comparison between model and measured values for the ratio $O_3/2H_2O_2+NO_z$ is especially important because it provides an indirect evaluation for the use of O_3/NO_z as a NO_x-VOC indicator. As stated above, the indicator hypothesis would interpret discrepancies between model and measured O_3/NO_z as evidence for erroneous NO_x-VOC sensitivity in the model. However, differences between model and measured O_3/NO_z can also be due to factors that have nothing to do with NO_x-VOC sensitivity, for example, deposition. The influence of these extraneous factors can be tested by comparing model and measured $O_3/2H_2O_2+NO_z$. This ratio is sensitive to model assumptions about deposition rates for H_2O_2 and HNO_3, but is relatively unaffected by the factors that determine NO_x-VOC sensitivity. In the current example, the small overestimate for $O_3/2H_2O_2+NO_z$ in the model suggests that model dry deposition may be underestimated, but it can also be used to limit the extent of the underestimate.

Sillman [1995] described the correlation between O_3 and $2H_2O_2+NO_z$ as the result of the balance between sources and sinks of odd hydrogen radicals ($OH+HO_2$ and analogous organic radicals, abbreviated RO_2), where radical sources increase in proportion with O_3 and accumulated sinks are represented by $2H_2O_2+NO_z$. This represents a significant change from previous interpretations of measured correlations involving O_3. Previous interpretations have emphasized the ozone production efficiency [*Liu et al.*, 1987; *Lin et al*., 1988] and the rate of production of O_3 as a function of precursors (NO_x, VOC, or CO [e.g., *Trainer et al.*, 1993; *Parrish et al.*, 1993]). The correlation between O_3 and $2H_2O_2+NO_z$ might be interpreted similarly as a production efficiency for O_3 as a function of odd hydrogen. However, *Sillman* [1995] interpreted the correlation in terms of the rate of production of $H_2O_2+NO_z$ rather than in terms of production of O_3. In this interpretation the correlation represents the rate of production of $H_2O_2+NO_z$ as a function of the O_3 concentration, where O_3 determines the availability of odd hydrogen. This interpretation would explain the linear correlation between O_3 and $2H_2O_2+NO_z$, and will be used as a working hypothesis throughout this analysis.

5.3. O_3 Versus $2(H_2O_2+ROOH)+NO_z$

In theory, the balance between sources and sinks of odd hydrogen should result in a linear correlation between O_3 and a sum that includes both H_2O_2 and organic peroxides (abbreviated throughout as "peroxides") rather than between O_3 and $2H_2O_2+NO_z$. Results in Figures 2 and 3 show that a correlation does exist between O_3 and 2peroxides+NO_z, but the scatter is greater than in the correlations for NO_z or for $2H_2O_2+NO_z$. In the model results the lower values for O_3/(2peroxides+NO_z) are found in locations with high isoprene and with a high ratio organic peroxides to H_2O_2. This result is apparently due to the difference in dry deposition rates between H_2O_2 and the organic peroxides. Since H_2O_2 deposits more rapidly than organic peroxides, the summed ambient concentration of peroxides should be larger when the sum consists largely of organic peroxides rather than H_2O_2. If deposition were not included in the model (see Figure 14 and section 8, below, also the statistics in Table 1), the scatter in the model correlation is greatly reduced. The scatter also may be due to the role of isoprene as a precursor for organic species (e.g. HCHO) that act as sources of odd hydrogen.

The model and measurements show excellent agreement for this correlation, both in terms of magnitude and in terms of the scatter. For low O_3 associated with the rural background the

model and measurements show a similar range of values for the peroxides-NO_z sum (2peroxides+NO_z=20-25 ppb for O_3=80 ppb). The model underestimates the peroxide-NO_z sum slightly for peak O_3 (27 modeled, 30 measured). The ratio O_3/(2peroxides+NO_z) shows a slight tendency to increase between rural (low O_3) and urban (high O_3) locations in both the model and in measurements (Figures 4 and 5), with similar values in the model and in measurements.

The model performance is somewhat worse if the peroxides are examined in isolation rather than as part of the peroxide-NO_z sum. A plot of peroxides versus NO_z (Figures 6 and 7) shows that the model underestimates organic peroxides associated with high NO_z in the Nashville urban plume (ROOH equal to 2.5 ppb in the model, 4.5 ppb measured, at NO_z=15 ppb). There is also a slight tendency to underestimate H_2O_2 in the model. Model organic peroxides agree with measurements for low NO_z. The specific model-measurement discrepancy for organic peroxides in the Nashville plume suggest the possibility that emission of anthropogenic VOC is underestimated. The scenarios with increased VOC would show better agreement with measured ROOH and total peroxides in the Nashville plume (ROOH equal to 4 ppb, total peroxides equal to 7 ppb at NO_z=15 ppb in this model scenario). Investigation of VOC emissions in comparison with measurements, including measured VOC, should be a subject of further study. It is also possible that organic peroxides are produced directly from the reaction of O_3 with isoprene [*Gäb et al.*, 1995; *Hewitt and Kok*, 1991; *Simonaitis et al*., 1991; see also *Enders et al.*, 1992]. No such production is included in the model.

5.4. Alternative Scenarios

As stated above, model-measurement discrepancies for O_3/NO_z might be explained either by assuming a higher loss rate for reactive nitrogen or by changing model assumptions that relate to NO_x-VOC sensitivity. These possibilities will be explored here.

Figures 8 and 9 show results of a model scenario with increased dry deposition (5 cm s^{-1}) for HNO_3 and H_2O_2. Results show a better agreement with measurements for O_3 versus NO_z and for O_3 versus $2H_2O_2$+NO_z. NO_z associated with both the rural background and the Nashville plume compare closely with measured values, and the O_3/NO_z ratio (Figure 9) compares well with measurements. The O_3-NO_z slope is still lower than in measurements (4.5 versus 5.7 measured, see Table 1). There is excellent agreement between model and measured O_3 versus $2H_2O_2$+NO_z, although the scenario tends to underestimate H_2O_2 (2-3 modeled, 3-4 measured at NO_z=5). The scenario also shows slightly worse agreement than the standard scenario for the sum 2peroxides+NO_z, with underestimates at both low and high O_3. Despite these minor discrepancies, the high-deposition scenario shows excellent overall agreement with the set of measured O_3, NO_z, and peroxides and represents an improvement over the standard scenario.

Scenarios with increased mixing heights (especially with a more rapid increase in mixing during the morning hours) and with increased emission rates for VOC also result in higher O_3/NO_z and better agreement with measurements. Scenarios with convective mixing heights derived from the RUC model rather than from local temperature soundings have O_3/NO_z increased by 10-20% relative to the standard model scenario at both urban and rural sites. The higher O_3/NO_z is accompanied by a greater sensitivity to NO_x rather than to VOC (see Table 2). Higher mixing heights tend to promote NO_x-sensitive chemistry [*Milford et al.*, 1994] and consequent higher O_3/NO_z. Increased vertical mixing during the morning also causes photochemical production of O_3 and NO_z to occur earlier in the day, resulting in faster removal of NO_z through deposition. However the scenarios with increased vertical mixing still tend to underestimate O_3/NO_z associated with low O_3 (O_3/NO_z<15 at O_3=80 ppb, versus 15-25 measured). O_3 versus $2H_2O_2$+NO_z and O_3 versus 2peroxides+NO_z are both comparable to the standard scenario; that is, O_3/$2H_2O_2$+NO_z is underestimated, but O_3 versus 2peroxides+NO_z agree well with measurements. Thus the scenario with increased mixing represents a plausible low-deposition scenario, although the scenario with high deposition appears more likely.

It is also useful to examine the impact of lower temperature on the predicted correlation between O_3, NO_z, and peroxides (Figure 10). At lower temperatures there is an increase in the net production of PAN, resulting in decreased ozone production efficiency on a per-NO_x basis and lower O_3-NO_z slope and O_3/NO_z ratio. At the same time, the source of odd hydrogen has been reduced due to lower H_2O and isoprene associated with the reduced temperature, causing an increase in the ratio O_3/2(H_2O_2+ROOH)+NO_z. NO_z becomes the dominant sink for odd hydrogen rather than peroxides, and there is a shift in the direction of VOC-sensitive chemistry. This shift associated with lower temperatures is consistent with the seasonal transition in NO_x-VOC chemistry described by *Jacob et al.* [1995].

5.5. Diurnal Variations

The diurnal variation in O_3/NO_z, O_3/$2H_2O_2$+NO_z, and O_3/2peroxides+NO_z (Figure 11) shows significant difference between urban Nashville and rural locations. The nighttime values of these ratios (representing conditions in the nocturnal boundary layer) reflects a complicated balance between surface deposition (especially of HNO_3 and H_2O_2), nighttime production of HNO_3, and, in an urban setting, removal of O_3 through reaction with emitted NO and NO_2. This results in nighttime minima in the vicinity of emission sources and maxima in rural sites. Ratios during the afternoon (between 1200 and 1800 LT) reflect diurnal variations in chemistry throughout the convective mixed layer rather than the impact of nighttime vertical mixing and entrainment during the morning hours. In downtown Nashville there is a significant increase in O_3/NO_z (from 1800 to 2100 LT) and a smaller increase in O_3/$2H_2O_2$+NO_z (from 1700 to 1800 LT) and O_3/2peroxides+NO_z (from 4.7 to 5.5) between 1200 and 1800 LT. A similar increase is predicted in rural locations. This increase is associated both with increased photochemical production of O_3, NO_z, and peroxides during the daytime (in contrast with nighttime production of HNO_3) and with deposition of HNO_3 and H_2O_2 as the air mass ages. The predicted change in O_3/NO_z and O_3/$2H_2O_2$+NO_z between 1200 and 1800 LT might be used as a basis for evaluating the impact of dry deposition on these ratios.

6. Evaluation of NO_x-VOC Indicators

Sillman [1995] showed that predicted O_3-NO_x-VOC sensitivity in models can be associated with certain "photochemical indicators," including O_3/NO_z, H_2O_2/NO_z, and several other ratios involving reactive nitrogen and peroxides. This section will present indicator-NO_x-VOC correlations in the model for Nashville, including the impact of updated photochemistry and deposition rates in comparison with results from *Sillman* [1995]. It will also use measured reactive nitrogen and peroxides as a basis for determining the indicator transition ratios. Use of measured indicator ratios to evaluate NO_x-VOC chemistry for Nashville will be presented in the next section.

Figure 12 shows the predicted change in O_3 concentrations resulting from either a 35% decrease in anthropogenic VOC or a 35% decrease in NO_x emissions in the standard scenario for Nashville, plotted against one of the indicator ratios (H_2O_2/NO_z). This figure illustrates the central properties of species that act as NO_x-VOC indicators. In the model, locations where O_3 shows greater sensitivity to NO_x than to VOC also have high values for H_2O_2/NO_z (>0.2). The few locations in which reduced VOC causes a significant reduction in O_3 also have the lowest H_2O_2/NO_z (<0.15). The simulations for Nashville show NO_x-sensitive chemistry in most of the model domain; only a few of locations (associated with peak O_3 in the Nashville urban plume) show sensitivity to VOC. The lowest model values for H_2O_2/NO_z in Figure 11 are representative of the region of transition between NO_x- and VOC-sensitive chemistry rather than strongly VOC-sensitive chemistry. Strongly VOC-sensitive simulations reported by *Sillman* [1995] and *Sillman et al.* [1997] include significantly lower H_2O_2/NO_z (<0.05).

A useful way to summarize the information in Figure 12 is to examine the percentile distribution of model indicator values for NO_x-sensitive and VOC-sensitive locations [*Sillman et al.*, 1997]. For this purpose, locations are defined as NO_x-sensitive at a given hour if the model predicts that a 35% reduction in NO_x would result in a reduction in O_3 of at least 5 ppb relative to both the initial scenario and to a simulation with a 35% reduction in VOC. Similarly, locations are defined as VOC-sensitive if a 35% reduction in anthropogenic VOC would result in a 5 ppb reduction in O_3 relative to both the initial and reduced-NO_x scenarios. The indicator values for NO_x-sensitive and VOC-sensitive locations (at the same hour as the NO_x-VOC sensitivity prediction) are then ranked by size and the percentile values for the indicator distribution (median, 95th percentile, etc.) are identified. The indicator-NO_x-VOC correlation can be summarized by four numbers: the median indicator value for VOC-sensitive locations; the 95th percentile value for VOC-sensitive locations; the 5th percentile value for NO_x-sensitive locations; and the median value for NO_x-sensitive locations. For an effective NO_x-VOC indicator, the median VOC-sensitive value is much lower than the median NO_x-sensitive value, and the 95th percentile VOC-sensitive value is equal to or lower than the 5th percentile NO_x-sensitive value. In these cases the 95th and 5th percentile values define the NO_x-VOC transition; that is, lower indicator values are associated with VOC-sensitive chemistry and higher values are associated with NO_x-sensitive chemistry.

Table 3 shows percentile values for three different indicators (O_3/NO_z, H_2O_2/NO_z and total peroxides/NO_z) for model scenarios with varying emission rates, chemistry, and dry deposition. Most of the scenarios in Table 3 include reduced biogenic emissions, equivalent to BEIS1, because these simulations have a larger VOC-sensitive region and consequently provide a more robust definition of the NO_x-VOC transition. In each case the 95th percentile VOC-sensitive indicator value is equal to or lower than the 5th percentile NO_x-sensitive value, demonstrating that the indicator successfully distinguishes NO_x- and VOC-sensitive chemistry. The median indicator value associated with VOC-sensitive chemistry differs only slightly from the 95th percentile value in these simulations. This similarity between the median and 95th percentile VOC-sensitive value occurs because the model has very little VOC-sensitive chemistry; so that even the median VOC-sensitive value is representative of the NO_x-VOC transition region. Results of simulations with strong VOC-sensitive chemistry, reported previously, showed a significant difference between median and 95th percentile VOC-sensitive values, equivalent in magnitude to the differences shown here between 5th percentile and median NO_x-sensitive values.

Results suggest that dry deposition represents the most important uncertainty for the indicator-NO_x-VOC predictions. The transition value for O_3/NO_z increases from 8 to 10 when the dry deposition velocity in the model is increased from 2.5 to 5 cm s^{-1} (standard versus D5 scenarios). The transition value for O_3/NO_z is also significantly lower when evaluated at noon as opposed to 1600 LT, and in scenarios with lower temperatures. The peroxide-based indicators (H_2O_2/NO_z and H_2O_2+ ROOH/NO_z) are less sensitive to deposition if deposition rates are assumed to be the same for H_2O_2 and HNO_3. However the transition value for H_2O_2/NO_z would increase if deposition rates were reduced for H_2O_2 but not for HNO_3 (scenario D1B). The peroxide-based indicators are also somewhat affected by time of day (noon versus 1600 LT) and temperature.

The NO_x-VOC transition points identified here for H_2O_2/NO_z are lower than the values reported by *Sillman* [1995] (0.15-0.20 in this study, 0.20-0.35 previously). Similar changes in NO_x-VOC transitions are found for other indicator ratios involving H_2O_2. These differences are associated with two changes in model assumptions between this study and *Sillman* [1995]: increased dry deposition rate for H_2O_2 (from 1 cm/s to 2.5 cm/s); and updated reaction rates for HO_2-RO_2 and RO_2-RO_2 reactions from *Kirchner and Stockwell* [1996]. Scenarios without these changes (D1B and Ch in Table 3) show higher transition values.

The resulting NO_x-VOC transition points for all indicators (with ranges representing the standard scenario and scenarios with high deposition and/or low biogenic emissions) are as follows: for O_3/NO_y, 6-8; for O_3/NO_z, 8-10; for O_3/HNO_3, 10-15; for H_2O_2/NO_y, 0.13-0.17; for H_2O_2/NOz, 0.15-0.20; and for H_2O_2/HNO_3, 0.20-30. Transition points for total peroxides are as follows: for peroxides/NO_y, 0.17-0.25; for peroxides/NO_z, 0.25-0.35; and for peroxides/HNO_3, 0.30-0.45.

This analysis represents the impact of reduced NO_x or VOC on ozone concentrations, which reflects chemistry over a multihour or multiday time period. *Sillman* [1995] and Kleinman et al. (1997) have identified a theoretical criteria for NO_x-VOC sensitivity associated with instantaneous production rates of ozone ($P(O_3)$). They found that $P(O_3)$ is sensitive to NO_x whenever production of peroxides (P(perox)) exceeded

production of HNO_3 ($P(HNO_3)$) as odd hydrogen sinks; that is, $[P(perox)/P(HNO_3)]>0.5$. This criteria for instantaneous chemistry should not be confused with the criteria for NO_x-VOC indicator transitions given above. The transition point for peroxides/HNO_3 is affected by many factors, including loss rates for peroxides and HNO_3 and the effect of nonlinear chemistry (i.e., peroxides/HNO_3 does not equal a linear sum of the instantaneous ratio $P(perox)/P(HNO_3)$ over the air mass history). The transition point for this and other indicator ratios is not necessarily the same as the criteria identified by Sillman and Kleinman et al. for instantaneous ozone production.

The predicted correlation between NO_x-VOC sensitivity and indicator ratios is difficult to test because there is no direct method for determining real-world NO_x-VOC sensitivity apart from model predictions. One way to evaluate the indicator-NO_x-VOC correlation is to examine cross correlations between different indicators (e.g., O_3/NO_z versus H_2O_2/NO_z) in comparison with measurements. This type of cross correlation is shown in Figures 13 and 14.

Results show that H_2O_2/NO_z and peroxides/NO_z both increase with O_3/NO_z in the model and in measurements. Little can be inferred from this successful cross correlation between indicator values because both indicators have NO_z in the denominator. However it is possible to evaluate the indicator NO_x-VOC transition points by comparing model values for H_2O_2/NO_z and peroxides/NO_z that are associated with O_3/NO_z between 9 and 10 (close to the NO_x-VOC transition for O_3/NO_z) with the equivalent measured values. This comparison tests whether the NO_x-VOC interpretation of the two measured indicator ratios is self-consistent; that is, both ratios indicating NO_x-sensitive chemistry, or both representing the NO_x-VOC transition, etc. In Figure 14, measured O_3/NO_z between 9 and 10 is associated with a specific value of H_2O_2/NO_z (=0.2) and peroxides/NO_z (=0.5). These measured crossover values must agree with the equivalent crossover values in models if the model NO_x-VOC transitions are correct. The model results (Figure 13) show that the standard scenario overestimates the crossover values for both H_2O_2/NO_z (=0.3) and peroxides/NO_z (=0.5-0.9). The model results also illustrate the tendency for the model to generate low O_3/NO_z relative to measurements throughout the domain. By contrast, the scenario with high deposition shows excellent agreement with measurements for both H_2O_2/NO_z (crossover equal to 0.2) and peroxides/NO_z (crossover equal to 0.45).

This type of model evaluation is closely related to the ratio $O_3/2H_2O_2+NO_z$, which was discussed in the previous section. This ratio can be expressed as a function of the NO_x-VOC transition associated with O_3/NO_z (T_o) and the NO_x-VOC transition associated with H_2O_2/NO_z (T_h) as follows:

$$\frac{O_3}{2H_2O_2 + NO_z} = \frac{T_o}{2T_h + 1} \qquad (1)$$

Thus agreement between models and measurements for $O_3/2H_2O_2+NO_z$ should guarantee that the indicator ratios O_3/NO_z and H_2O_2/NO_z are consistent with each other. Similarly, agreement between modeled and measured O_3/2peroxides+NO_z suggests self-consistency of O_3/NO_z and peroxides/NO_z as NO_x-VOC indicators.

7. NO_x-VOC Sensitivity for Nashville

Analysis of NO_x-VOC sensitivity for Nashville will be based on predictions of the various model scenarios and on comparisons between modeled and measured indicator ratios (O_3/NO_z, H_2O_2/NO_z and peroxides/NO_z). As described in section 2 the model scenarios were designed to include a range of NO_x-VOC predictions, with the intent of using measurements to evaluate the accuracy of the different scenarios. NO_x-VOC predictions and indicator ratios for the model scenarios are summarized in Table 2.

Figures 15 and 16 show H_2O_2/NO_z and peroxides/NO_z versus O_3 in the standard model scenario and in measurements. The model and measurements both show a distinction between high H_2O_2/NO_z and peroxides/NO_z associated with relatively low O_3, representing the rural background, and low H_2O_2/NO_z and peroxides/NO_z associated with high O_3, representing the Nashville urban plume. A similar geographical variation is found for O_3/NO_z for low and high O_3 (see Figures 4 and 5).

The geographical variation in indicator ratios might be interpreted to represent the difference between NO_x-sensitive chemistry in rural locations and greater sensitivity to VOC in the Nashville urban plume. However results from both models and measurements suggest that the indicator ratios in Nashville represent transitional chemistry rather than VOC-sensitive chemistry. As shown previously (Figure 12), the lowest values of indicator ratios in the standard scenario are associated with the NO_x-VOC transition. In addition, the measured indicator ratios concurrent with peak O_3 all show values that are close to the NO_x-VOC transitions identified in the previous section (O_3/NO_z=9, H_2O_2/NO_z=0.20). Measured total peroxides/NO_z (=0.44) would suggest NO_x-sensitive chemistry even in the urban plume.

As was done previously by *Sillman et al.* [1995, 1997], we will evaluate individual model scenarios by comparing indicator ratios associated with peak O_3 in the model with indicator ratios associated with measured peak O_3, not necessarily in the same location as the model peak. Results (Table 2) show that the standard scenario gives values that are lower than measurements for all three indicator ratios. The underestimate is relatively small for O_3/NO_z but is larger for H_2O_2/NO_z and peroxides/NO_z, and suggests that the scenario is biased toward VOC-sensitive chemistry. Referring to Figures 4-5 and 15-16, it appears that the underestimated indicator ratios are associated specifically with a small number of model locations (all in the Nashville urban center) with lower indicator ratios than the rest of the model domain. These locations with low indicator ratios also show greater sensitivity to VOC than the rest of the model domain.

Peak O_3 in the model occurs at 1600 rather than at 1400 LT, and the subsequent discussion will refer to predicted O_3-NO_x-VOC sensitivity at the time of peak O_3. The standard scenario predicts that peak O_3 shows equal sensitivity to reduced NO_x and VOC, although the impact of reduced NO_x is due in part to upwind NO_x sources rather than to emissions in Nashville. The impact of reduced VOC in the simulations is due almost entirely to reduced emissions in Nashville rather than upwind.

Table 2 also shows that relatively small changes in model assumptions cause large changes in predicted NO_x-VOC sensitivity for peak O_3. In the scenario with RUC mixing

heights peak O_3 shows greater sensitivity to NO_x then to VOC. Simulations for July 12 and (especially) July 18 also show greater sensitivity to NO_x than to VOC. This change in NO_x-VOC sensitivity occurs because greater dispersion (through winds and vertical mixing) tends to create NO_x-sensitive chemistry while stagnant conditions tend to create VOC-sensitive chemistry [*Milford et al.*, 1994; see also *Kleinman*, 1994]. Scenarios with increased VOC emissions also show NO_x-sensitive chemistry, while the scenarios with reduced biogenic VOC (equivalent to the BEIS1 inventory) show VOC-sensitive chemistry. The NO_x-sensitive model scenarios also have higher indicator ratios while the VOC-sensitive scenarios have lower indicator ratios. By contrast, the ratios $O_3/(2H_2O_2+NO_z)$ and $O_3/(2\text{peroxides}+NO_z)$ are affected by model deposition rates but show little change in response to changed model NO_x-VOC sensitivity.

The best agreement with measured indicator ratios is found in the NO_x-sensitive scenarios, especially in the scenarios with increased VOC emissions. However there is no strong basis for rejecting the standard scenario (with equal sensitivity to NO_x and VOC) since the low indicator ratios in this scenario are associated with a small number of model locations, which could easily have been missed in the aircraft flight path.

It is useful to contrast the measured O_3/NO_z (=9.3) and H_2O_2/NO_z (=0.2) associated with peak O_3 in Nashville on July 13 with previously measured indicator ratios in Atlanta [*Sillman*, 1995; *Sillman et al.*, 1995] and Los Angeles [*Sillman*, 1995; Sillman *et al.*, 1997]. The measured values in Atlanta (O_3/NO_y=14) are associated with NO_x-sensitive chemistry, while measurements in Los Angeles (O_3/NO_z=4-6, H_2O_2/NO_z=0.03) are associated with VOC-sensitive chemistry. The Nashville measurements represent intermediate values between NO_x-sensitive Atlanta and VOC-sensitive Los Angeles. They also represent intermediate values between measured values in rural Virginia associated with a seasonal transition between NO_x- and VOC-sensitive chemistry [*Jacob et al.*, 1995]. The indicator values in Nashville may be seen as representative of chemistry close to the NO_x-VOC transition.

Results for July 18 deserve special notice. This day was characterized by high winds (5 m/s) relatively low O_3, and chemistry that closely resembles rural sites even in the Nashville urban plume. Simulations for this day show high O_3/NO_z and H_2O_2/NO_z, both characteristic of NO_x-sensitive chemistry. Measured O_3/NO_z (=12) is consistent with model results and also suggests NO_x-sensitive chemistry. However the measured H_2O_2 was very low (<1 ppb) and significant discrepancies appear between model and measured values for H_2O_2/NO_z (model equal to 0.41, measurement equal to 0.16) and $O_3/2H_2O_2+NO_z$ (model equal to 6.5, measurement equal to 9.6). The measured indicator ratios (O_3/NO_z and H_2O_2/NO_z) give contradictory values for NO_x-VOC chemistry. These measurements can be reconciled with model results only if an unspecified upwind loss for H_2O_2, possibly through wet deposition or aqueous chemistry, is assumed.

8. Ozone Production Efficiency and Removal Processes

In the previous discussion of correlations between O_3 and NO_z and between O_3, NO_z, and peroxides, it was assumed that the correlations were determined primarily by photochemical production, production of ozone in association with the O_3-NO_z correlation, and production of NO_z and peroxides as odd hydrogen sinks in association with the correlation between O_3, NO_z, and peroxides. There has already been extensive analysis of the correlation between O_3 and NO_z in this context. The slope $\Delta O_3/\Delta NO_z$ has been associated with the ozone production efficiency, that is, the ratio of the rate of production of ozone ($P(O_3)$) to the loss rate of NO_x ($L(NO_x)$) [*Liu et al.*, 1987; *Lin et al.*, 1988; *Trainer et al.*, 1993; *Olszyna et al.*, 1994; *Kleinman et al.*, 1994]. *Chin et al.* [1994], *Jacob et al.* [1995] and Ryerson (this issue) have suggested that the observed correlation between O_3 and NO_z may be largely influenced by photochemical losses of O_3 and NO_z rather than production. P. H. Daum (private communication, 1997) has also found instances in which the observed $\Delta O_3/\Delta NO_z$ does not represent the true ozone production efficiency because it represents the difference between two air parcels with different photochemical age and history. There has also been confusion over the use of $\Delta O_3/\Delta NO_z$ as evidence for NO_x-VOC chemistry. Initially, *Sillman et al.* [1990b] suggested that a positive correlation between O_3 and total reactive nitrogen (NO_y) could be interpreted as evidence for NO_x-sensitive chemistry, but more recent results [*Sillman*, 1995] suggested that the O_3/NO_z ratio, not the slope, should be used to identify NO_x-VOC chemistry.

In order to investigate the relative impact of photochemical production and losses on these correlations, the Nashville standard scenario has been repeated with all photochemical losses for NO_z and peroxides removed, except for thermal decomposition of PAN and equivalent organic nitrates. Dry deposition losses were also eliminated for all species, including O_3. Photochemical losses for O_3 were retained. In this modified scenario the ratio (O_3-40ppb)/NO_z represents the exact net ozone production efficiency, $[P(O_3)-L(O_3)]/L(NO_x)$ for each air parcel, averaged over the history of the air parcel. Correlations between O_3, NO_z, and peroxides for this modified scenario are shown in Figure 17.

Net ozone production efficiency in this scenario is approximately 3 in both the Nashville urban plume (O_3=130, NO_z=30) and in rural air (O_3=80, NO_z=12-17). These values reflect photochemistry in association with 1-4 ppb NO_x during the daytime. If ozone production efficiency were defined as $[P(O_3)-L(O_3)]/P(HNO_3)$, as by *Liu et al.* [1987] and *Lin et al.* [1988], the resulting values would be 25% higher (4-5 rather than 3-4). Somewhat higher values would also be found if ozone production efficiency were calculated for the daytime only, ignoring nighttime loss of NO_x.

These ozone production efficiencies are significantly lower than the values derived from the slope between O_3 and NO_z in the standard model scenario. Referring to Figure 3, the concentrations of O_3 and NO_z in photochemically aged rural air (O_3=80 ppb, NO_z=6-10 ppb) would imply a slope of 4-7 relative to the model background (O_3=40 ppb, NO_z=0). For the Nashville urban plume (peak O_3=135, NO_z=19) relative to photochemically aged rural air the slope between O_3 and NO_z is 5. For both the Nashville urban plume and photochemically aged rural air the true ozone production efficiency (relative to $L(NO_x)$) is 40% lower than the value that would be derived from O_3 versus NO_z in the standard model scenario, if the analysis of

O_3 versus NO_z did not account for loss of NO_z. A similar difference is found in the calculated slope between O_3 and NO_z in Table 1 (standard scenario equal to 4.0, zero-loss scenario 2.8). If results from the scenario with high deposition were assumed, the difference between O_3-NO_z slope and ozone production efficiency would be even larger.

The ozone production efficiencies shown here are higher than the estimate (equal to 1.7) derived by *Chin et al.* [1994], from correlations between O_3 and CO. However, the calculation by Chin et al. was based on CO and NO_x emissions reported by the NAPAP 1985 inventory [*EPA*, 1989]. Subsequent inventories [*EPA*, 1993] reported CO emissions that were higher than the previous estimate by 50%. If this higher emission estimate were added to the analysis of *Chin et al.* [1994], the resulting ozone production efficiency would be 2.6, a value which is consistent with this analysis. *Hirsch et al.* [1996] reported a similar value (equal to 2.9) based on measured O_3 and CO in Massachusetts. The range of ozone production efficiencies shown here is also consistent with the values reported by *Jacob et al.* [1993] in a model for the eastern United States (equal to 4.4), although a more recent calculation by *Hirsch et al.* [1996] reported significantly higher values (equal to 5.7).

It is also useful to compare the ozone production efficiencies associated with the Nashville urban plume, the relatively small Gallatin power plant, and the larger Cumberland power plant in these simulations. Peak O_3 associated with Nashville in the zero-loss scenario for July 13 (equal to 143 ppb at 1600 LT) is higher than peak O_3 associated with the power plant plumes (equal to 115 ppb for Gallatin, 111 ppb for Cumberland). However the ozone production efficiency, defined as $[P(O_3)-L(O_3)]/L(NO_x)$ is similar between Nashville (equal to 3.2), the Gallatin plume (equal to 3.6), and the upwind rural region (equal to 3.6). The Cumberland plume has lower ozone production efficiency (equal to 2.0). On July 12, ozone production efficiency in the Cumberland plume is closer to the values elsewhere (equal to 2.8 for Cumberland, 3.6 for Nashville and the upwind rural region). On July 18, a day with stronger winds (4-5 m s^{-1}) simulated NO_x is lower both in rural areas and in Nashville, and ozone production efficiencies are higher (equal to 5), while in the Cumberland plume, ozone production efficiencies are unchanged (equal to 2-3).

The correlations between O_3, NO_z, and total peroxides in the scenario with zero photochemical losses show several interesting features. In the initial discussion (section 4), it was pointed out that the linear correlation between O_3 and the sums ($2H_2O_2+NO_z$) and (2peroxides+NO_z) can be interpreted as reflecting the balance between radical sources (proportional to O_3) and sinks (proportional to 2peroxides+NO_z). This interpretation is also consistent with the tendency for the ratio O_3/(2peroxides+NO_z) to have similar values in rural and urban locations. However the interpretation is somewhat imperfect because O_3 is associated with the rate of production of radicals whereas (2peroxides+NO_z) represents the accumulated loss of radicals over time. In the scenario with zero losses there is still a linear correlation between O_3 and ($2H_2O_2+NO_z$) and between O_3 and (2peroxides+NO_z), but the correlation no longer has an intercept near the origin and the ratio O_3/(2peroxides+NO_z) increases with increasing O_3 (i.e., is higher in urban locations). This change in the ratio O_3/(2peroxides+NO_z) reflects the above imperfection, where O_3 is associated with the rate of radical production on the 4th day (at the end of the simulation), while the sum (2peroxides+NO_z) represents the accumulation of radicals, without losses, over the entire 4-day period. The near-constant value for $O_3/2H_2O_2+NO_z$ and O_3/2peroxides+NO_z, found in both the standard model scenario and measurements, is apparently due to the fact that O_3, peroxides, and NO_z all have significant losses with similar (1-3 day) lifetimes.

Another feature of the correlation between O_3 and (2peroxides+NO_z) is the reduction in scatter in the scenario with zero losses as opposed to the standard model scenario (R_2=0.45 in the standard scenario, 0.39 with zero losses, see Table 1). This reduction in scatter between the standard and zero-loss scenarios only occurs for O_3 versus (2peroxides+NO_z), not for O_3 versus NO_z or O_3 versus ($2H_2O_2+NO_z$). In section 4 it was hypothesized that scatter in the correlation O_3 versus (2peroxides+NO_z) was due to the difference in loss rates between H_2O_2 and the organic peroxides. The reduced scatter in the scenario with zero losses supports this hypothesis.

9. Conclusions

This paper has examined correlations between O_3, NO_z, and peroxides, using both photochemical models and measurements from the Middle Tennessee Ozone Study, with special emphasis on the use of these species as photochemical indicators for O_3-NO_x-VOC chemistry. Results have been largely consistent with the original analysis of NO_z and peroxides as photochemical indicators [*Sillman*, 1995], but there have also been significant revisions of the NO_x-VOC transition values and some measurements (on July 18) that are contrary to theory. A linear correlation was found between O_3 and the sum $2H_2O_2+NO_z$, which is consistent with model results and with previous theoretical analyses [*Sillman*, 1995] and measurements [*Daum et al.*, 1996; *Staffelbach et al.*, 1997a, b]. This linear correlation provides evidence in support of the use of O_3/NO_z and $H_2O_2+NO_z$ as NO_x-VOC indicators, and also suggests that the NO_x-VOC transition value associated with O_3/NO_z in models is correct. A similar correlation has been found between O_3 and the sum $2H_2O_2$+2ROOH+NO_z, but with greater scatter. The modified NO_x-VOC transition values are consistent with cross correlations between measured O_3/NO_z and H_2O_2/NO_z in Nashville on July 11 and July 13 and are also consistent with measured O_3/NO_z and $H_2O_2+NO_z$ reported by *Staffelbach et al.* [1997a].

Deposition rates for HNO_3 and H_2O_2 provide a major source of uncertainty. We have found that the measured correlation between O_3, NO_z, and peroxides is consistent with model results with a dry deposition velocities of 5 cm s^{-1} and have derived indicator NO_x-VOC results based on these values. Deposition is also a major factor when measured O_3 and NO_z are used to infer ozone production efficiencies. The ozone production efficiency in models for Nashville (equal to 3) is significantly lower than the equivalent slope between O_3 and NO_z (equal to 4-7).

The measured indicator ratios in the Nashville urban plume (O_3/NO_z and $H_2O_2+NO_z$) are close to the values associated with the transition between NO_x- and VOC-sensitive chemistry in photochemical models. These transitional values form an intermediate point between previous measurements in Atlanta

and in rural areas (suggesting NO_x-sensitive chemistry) and Los Angeles (suggesting VOC-sensitive chemistry). The best agreement between model and measured indicator ratios was found in a NO_x-sensitive model scenario, but there were also plausible model scenarios in which peak O_3 showed equal sensitivity to NO_x and VOC and greater sensitivity to local VOC than to local NO_x. This model-measurement comparison does not provide a firm basis for accepting the NO_x-sensitive scenarios and rejecting the scenarios with mixed NO_x-VOC sensitivity. Similarly, the measured indicator ratios tended to be on the NO_x-sensitive side of model NO_x-VOC transition, but they are too close to the transition region to draw any definite conclusions.

Finally, it is important to recognize the limited nature of the model-measurement comparisons shown here. A thorough analysis should include model evaluation in comparison with the extensive field measurements of VOC in Nashville. This is especially important because the uncertainty in model NO_x-VOC predictions is associated largely with uncertainties in emission rates for VOC. Comparison with measured VOC would provide an additional basis for evaluating model scenarios with different NO_x-VOC chemistry. In the absence of a comparison between model and measured VOC, the VOC-NO_x predictions reported here must be regarded as tentative.

Acknowledgments. Discussions with Brad Hall, David Parrish, Stu McKeen, Tom Ryerson and Gail Tonneson were especially helpful in preparing this manuscript. We are indebted to Tom Ryerson for alerting us to the various uncertainties associated with ozone production efficiencies and other inferences from measured species correlations. This research is part of the Southern Oxidants Study (SOS)--a collaborative university, government, and private industry study to improve scientific understanding of the accumulation and effects of photochemical oxidants. Financial and in-kind support for SOS research and assessment activities is provided by the Environmental Protection Agency, National Oceanic and Atmospheric Administration, Department of Energy, Tennessee Valley Authority, Electric Power Research Institute, The Southern Company, Coordinating Research Council, and the States of Alabama, Florida, Georgia, Kentucky, Louisiana, Mississippi, North Carolina, South Carolina, Tennessee, and Texas. Although the research described in this article has been funded wholly or in part by the Environmental Protection Agency under Assistance Agreement No. CR818336 to University of Alabama in Huntsville, it has not been subjected to the Agency's peer and administrative review, and therefore may not necessarily reflect the views of the Agency, and no official endorsement should be inferred. Additional support was provided by the National Science Foundation for measurement of peroxides (ATM-9414108) and for modeling and interpretation (ATM-9713567).

References

Andronache, C., W. L. Chameides, M. O. Rodgers, J. E. Martinez, P. Zimmerman, and J. Greenberg. Vertical distribution of isoprene in the lower boundary layer of the rural and urban southern United States, *J. Geophys. Res.*, *99*, 16,989-17,000, 1994.

Benjamin S. G., K. J. Brundage and L. L. Morone, Implementation of the Rapid Update Cycle, I, Analysis/model description, *NOAA/NWS Tech. Procedures Bull. Ser. 416*, Natl. Oceanic and Atmos. Admin., Silver Spring, Md., 1994.

Bollinger, M. J., R. E. Sievers, D. W. Fahey, and F. C. Fehsenfeld, Conversion of nitrogen dioxide, nitric acid and n-propyl nitrate to nitric oxide by gold-catalyzed reduction with carbon monoxide, *Anal. Chem.*, *55*, 1980-1986, 1983.

Chin, M., D. J. Jacob, J. W. Munger, D. D. Parrish, and B. G. Doddridge, Relationship of ozone and carbon monoxide over North America, *J. Geophys. Res.*, *99*, 14,565-14,573, 1994.

Daum, P. H., L. I. Kleinman, L. Newman, W. T. Luke, J. Weinstein-Lloyd, C. M. Berkowitz, and K. M. Busness, Chemical and physical properties of anthropogenic pollutants transported over the North Atlantic during NARE, *J. Geophys. Res.*, *101*, 29,029-29,042, 1996.

DeMore, W. B., S. P. Sander, D. M. Golden, R. F. Hampson, M. J. Kurylo, C. J. Howard, A. R. Ravishankara, C. E. Kolb, and M. J. Molina, Chemical kinetics and photochemical data for use in stratospheric modeling, *JPL Publ.*, *94-26*, 1994.

Enders, G., et al., Biosphere /atmosphere interactions: Integrated research in a European coniferous forest ecosystem, *Atmos. Environ., Part A, 26A*, 171-189, 1992.

Environmental Protection Agency (EPA), The 1985 NAPAP emissions inventory (version 2): Development of the annual data and modelers' tapes, *EPA-600/7-89-012a*, Environ. Prot. Agency, Research Triangle Park, N. C., 1989.

Environmental Protection Agency (EPA), Regional interim emission inventories (1987-1991), vols. 1 and 2, *EPA-454/R93-021a and b*, Environ. Prot. Agency, Research Triangle Park, N. C., 1993.

Flowers, E. C., R. A. McCormick, and K. R. Kurfis, Atmospheric turbidity over the United States, 1961-1966, *J. Appl. Meteorol.*, *8*, 955-962, 1969.

Fujita, E. M., B. E. Croes, C. L. Bennett, D. R. Lawson, F. W. Lurmann, and H. H. Main, Comparison of emission and ambient concentration ratios of CO, NO_x, and NMOG in California's south coast air basin, *J. Air Waste Manage. Assoc.*, *42*, 264-276, 1992.

Gäb, S., W. Turner, S. Wolff, K. Becker, L. Rupert, and K. Brockman, Formation of hydroxyalkyl hydroperoxides on ozonolysis in water and air, *Atmos. Environ.*, *29*, 2401- 2407, 1995.

Gao, D., W. R. Stockwell, and J. B. Milford, Global uncertainty analysis of a regional-scale gas phase chemical mechanism, *J. Geophys. Res.*, *101*, 9071-9078, 1996.

Geron, C. D., A. B. Guenther, and T. E. Pierce, An improved model for estimating emissions of volatile organic compounds from forests in the eastern United States, *J. Geophys. Res.*, *99*, 12,773-12,791, 1994.

Hall, B. D., and C. S. Claiborn, Measurements of the dry deposition of peroxides to a Canadian boreal forest, *J. Geophys. Res.*, *102*, 29,343-29,353, 1997.

Heffter, J. L., Air resources laboratories atmospheric transport and dispersion model, *NOAA Tech. Memo, ERL ARL-81*, 24 pp., Natl. Oceanic and Atmos. Admin., Silver Springs, Md., 1980.

Hewitt, C. N., and G. L. Kok, Formation and occurrence of organic peroxides in the troposphere: Laboratory and field observations, *J. Atmos. Chem. 12*, 181-194, 1991.

Hirsch, A. I., J. W. Munger, D. J. Jacob, L. W. Horowitz, and A. H. Goldstein, Seasonal variation of the ozone production efficiency per unit NO_x at Harvard Forest, Massachusetts, *J. Geophys. Res.*, *101*, 12,659-12,666, 1996.

Hubler, G., R. Alvarez, P. Daum, R. Dennis, N. Gillani, L. Kleinman, W. Like, J. Meagher, D. Rider, M. Trainer, and R. Valente, An overview of the airborne activities during the 1995 summer intensive of the Southern Oxidants Study in Nashville, Tennessee, *J. Geophys. Res.*, this issue.

Jacob, D. J., and S. C. Wofsy, Photochemistry of biogenic emissions over the Amazon forest, *J. Geophys. Res.*, *93*, 1477-1486, 1988.

Jacob, D. J., J. A. Logan, G. M. Gardner, R. M. Yevich, C. M. Spivakowsky, S. C. Wofsy, S. Sillman, and M. J. Prather, Factors regulating ozone over the United States and its export to the global atmosphere, *J. Geophys. Res.*, *98*, 14,817-14,827, 1993.

Jacob, D. J., B. G. Heikes, R. R. Dickerson, R. S. Artz, and W. C. Keene, Seasonal transition from NO_x- to hydrocarbon-limited ozone production over the eastern United States in September, *J. Geophys. Res.*, *100*, 9315-9324, 1995.

Kirchner, F., and W. R. Stockwell, The effect of peroxy radical reactions on the predicted concentrations of ozone, nitrogenous compounds, and radicals, *J. Geophys. Res.*, *101*, 21,007-21,023, 1996.

Kleinman, L. I., Low- and high-NO_x tropospheric photochemistry, *J. Geophys. Res.*, *99*, 16,831-16,838, 1994.

Kleinman, L. I., Y-N. Lee, S. R. Springston, L. Nunnermacker, X. Zhou, R. Brown, K. Hallock, P. Klotz, D. Leahy, J. H. Lee, and L. Newman, Ozone formation at a rural site in the southeastern United States, *J. Geophys. Res.*, *99*, 3469-3482, 1994.

Kleinman, L. I., P. H. Daum, J. H. Lee, Y-N. Lee, L. J. Nunnermacker, S. R. Springston, L. Newman, J. Weinstein-Lloyd, and S. Sillman, Dependence of ozone production on NO and hydrocarbons in the troposphere, *Geophys. Res. Lett.*, *24*, 2299-2302, 1997

Kumar, N., and A. Russell, Development of a computationally efficient, reactive subgrid-scale plume model and the impact on the northeastern United States using increasing levels of chemical detail, *J. Geophys. Res*., *101*, 16,737-16,744, 1996.

Lee, J. H., I. N. Tang, and J. B. Weinstein-Lloyd, Nonenzymatic method for the determination of hydrogen peroxide in atmospheric samples. *Anal. Chem.*, *62*, 2381-2384, 1990.

Lee, J. H., D. F. Leehy, I. N. Tang, and L. Newman, Measurement and speciation of gas phase peroxides in the atmosphere, *J. Geophys. Res*., *98*, 2911-2915, 1993.

Lee, J. H., I. N. Tang, J. B. Weinstein-Lloyd, and E. B. Halper, An improved nonenzymatic method for the determination of gas-phase peroxides, *Environ. Sci. Technol.*, *28*, 1180-1185, 1994.

Lin, X., M. Trainer, and S. C. Liu, On the nonlinearity of tropospheric ozone, *J. Geophys Res*., *93*, 15,879-15,888, 1988.

Liu, S. C., M. Trainer, F. C. Fehsenfeld, D. D. Parrish, E. J. Williams, D. W. Fahey, G. Hubler, and P. C. Murphy, Ozone production in the rural troposphere and the implications for regional and global ozone distributions, *J. Geophys. Res.*, *92*, 4191-4207, 1987.

Lurmann, F. W., A. C. Lloyd, and R. A. Atkinson, Chemical mechanism for use in long-range transport/acid deposition computer modeling, *J. Geophys. Res.*, *91*, 10,905-10,936, 1986.

Madronich, S., Photodissociation in the atmosphere, 1, Actinic flux and the effect of ground reflections and clouds, *J. Geophys. Res.*, 92, 9740-9752, 1987.

Marsik, F. J., K. W. Fischer, T. D. McDonald, and P. J. Samson, Comparison of methods for estimating mixing heights used during the 1992 Atlanta field intensive, *J. Appl. Meteorol.*, *45*, 8, 1995.

McNider, R. T., W. B. Norris, A. J. Song, R. L. Clymer, S. Gupta, R. M. Banta, R. J. Zamora, A. B. White, and M. Trainer, Meteorological conditions during the 1995 summer intensive of the Southern Oxidants Study in Nashville, Tennessee, *J. Geophys. Res.*, this issue.

Meagher, J. F., E. B. Cowling, F. C. Fehsenfeld, and W. J. Parkh, Ozone formation and transport in the southeastern United States: An overview of the 1995 summer intensive of the Southern Oxidants Study in Nashville, Tennessee, *J. Geophys. Res.*, this issue.

Milford, J., D. Gao, S. Sillman, P. Blossey, and A. G. Russell, Total reactive nitrogen (NO_y) as an indicator for the sensitivity of ozone to NO_x and hydrocarbons, *J. Geophys. Res*., *99*, 3533-3542, 1994.

Olszyna, K. J., E. M. Bailey, R. Simonaitis, and J. F. Meagher, O_3 and NO_y relationships at a rural site, *J. Geophys. Res.*, *99*, 14,557-14,563, 1994.

Parrish, D. D., J. S. Holloway, M. Trainer, P. C. Murphy, G. L. Forbes, and F. C. Fehsenfeld, Export of North American ozone pollution to the North Atlantic Ocean, *Science*, *259*, 1436-1439, 1993.

Paulson, S. E., and J. H. Seinfeld, Development and evaluation of a photooxidation mechanism for isoprene, *J. Geophys. Res.*, *97*, 20,703-20,715, 1992.

Prather, M. J., Numerical advection by conservation of second-order moments, *J. Geophys Res.*, *91*, 6671-6681, 1986.

Ryerson, T. B., M. P. Buhr, G. Frost, P. D. Goldan, J. S. Holloway, G. Hubler, B. T. Jobson, W. C. Kuster, S. A. McKeen, D. D. Parrish, J. M. Roberts, D. T. Sueper, M. Trainer, J. Williams, and F. C. Fehsenfeld, Emissions lifetimes and ozone formation in power plant plumes, *J. Geophys. Res*., this issue.

Sillman, S., The use of NO_y, H_2O_2 and HNO_3 as indicators for O_3-NO_x-VOC sensitivity in urban locations, *J. Geophys. Res.*, *100*, 14,175-14,188, 1995.

Sillman, S., J. A. Logan, and S. C. Wofsy, A regional-scale model for ozone in the United States with subgrid representation of urban and power plant plumes, *J. Geophys. Res.*, *95*, 5731-5748, 1990a.

Sillman, S., J. A. Logan, and S. C. Wofsy, The sensitivity of ozone to nitrogen oxides and hydrocarbons in regional ozone episodes, *J. Geophys. Res*., *95*, 1837-1851, 1990b.

Sillman, S., P. J. Samson, and J. M. Masters, Ozone production in urban plumes transported over water: Photochemical model and case studies in the northeastern and Midwestern United States, *J. Geophys. Res*., *98*, 12,687-12,699, 1993.

Sillman, S., et al., Photochemistry of ozone formation in Atlanta, GA: Models and measurements, *Atmos. Environ*., *29*, 3055-3066, 1995.

Sillman, S., D. He, C. Cardelino, and R. E. Imhoff, The use of photochemical indicators to evaluate ozone-NO_x-hydrocarbon sensitivity: Case studies from Atlanta, New York and Los Angeles, *J. Air Waste Manage. Assoc.*, *47*, 1030-1040, 1997.

Simonaitis, R., K. J. Olszyna, and J.F. Meagher, Production of hydrogen peroxide and organic peroxides in the gas phase reactions of ozone with natural alkenes, *Geophys. Res. Lett*., *18*, 9-12, 1991.

Singh, H. B., D. O'Hara, D. Herlth, J. D. Bradshaw, S. T. Sandholm, G. L. Gregory, W. Sachse, D. R. Blake, P. J. Crutzen, and M. Kanakidou, Atmospheric measurements of peroxyacetyl nitrate and other organic nitrates at high latitudes: Possible sources and sinks, *J. Geophys. Res.*, *97*, 16,511-16,522, 1992.

Smolarkiewicz, P. K., A simple positive definite advection scheme with small implicit diffusion, *Mon. Weather Rev.*,*111*, 479-486, 1983.

Staffelbach, T., et al., Photochemical oxidant formation over southern Switzerland, 1, Results from summer, 1994, *J. Geophys. Res*., *102*, 23,345-23,362, 1997a.

Staffelbach, T., A. Neftel, and L. W. Horowitz, Photochemical oxidant formation over southern Switzerland, 2, Model results, *J. Geophys. Res*., *102*, 23,363-23,373, 1997b.

Stockwell, W. R., F. Kirchner, and M. Kuhn, A new mechanism for regional atmospheric chemistry modeling, *J. Geophys. Res*., 102, 25,847-25,879, 1997.

Trainer, M., et al., Correlation of ozone with NO_y in photochemically aged air, *J. Geophys. Res*., *98*, 2917-2926, 1993.

Weinstein-Lloyd, J. B., J. H. Lee, P. H. Daum, L. Kleinman, L. J. Nunnermacker, S.R. Springston, and L. Newman, Measurements of peroxides and related species during the 1995 Summer intensive of the Southern Oxidants Study in Mashville, Tennessee, *J. Geophys. Res.*, this issue.

Williams, E. J., et al., Intercomparison of ground-based NO_y measurement techniques, *J. Geophys. Res.*, in press, 1998.

P. H. Daum, D. G. Imre, L. I. Kleinman, and J. H. Lee, Environmental Chemistry Division, Brookhaven National Laboratories, Upton, NY 11973-5000. (e-mail: phdaum@bnl.gov; imre@bnl.gov; kleinman@bnl.gov; jaihlee@bnl.gov)

D. He, M. R. Pippin, and S. Sillman, Department of Atmospheric, Oceanic, and Space Sciences, University of Michigan, 2455 Hayward St., Ann Arbor, MI 48109-2143. (e-mail: dyhe@engin.umich.edu; pippin@engin.umich.edu; sillman@umich.edu)

J. Weinstein-Lloyd, Chemistry/Physics Department, State University of New York, Old Westbury, NY 11568-0210. (e-mail: jlloyd@bnl.gov)

Table 1. Linear Least Square Estimates for O_3-NO_z-Peroxide Correlations

	a_0	a_1	r_2	Ratio
	O_3 Versus NO_z			
Measurements (Figure 2)	60	5.7	0.90	16.1
Standard model (Figure 3	56	4.0	0.85	9.9
High deposition (Figure 8)	61	4.5	0.85	13.0
Low temperature (Figure 10)	47	3.0	0.82	7.3
Zero deposition (Figure 17)	46	2.8	0.85	5.3
	O_3 Versus ($2H_2O_2$+NO_z)			
Measurements (Figure 2)	11	6.4	0.93	7.3
Standard model (Figure 3	23	4.5	0.89	6.1
High deposition (Figure 8)	34	5.0	0.90	7.8
Low temperature (Figure 10)	29	3.6	0.84	5.8
Zero deposition (Figure 17)	-12	3.0	0.89	2.7
	O_3 Versus (2peroxides+ NO_z)			
Measurements (Figure 2)	-8	4.5	0.78	4.2
Standard model (Figure 3	-54	6.2	0.45	4.0
High deposition (Figure 8)	-39	6.6	0.39	4.6
Low temperature (Figure 10)	-2	4.8	0.63	4.7
Zero deposition (Figure 17)	-136	4.3	0.71	1.8

Intercept (a_0), slope (a_1), and correlation coefficient (r^2) are shown for O_3 as a function of NO_z, $2H_2O_2$+NO_z, and 2peroxides+NO_z (i.e., for $[O_3]=a_0+a_1[NO_z]$, etc.) in Figures 2, 3, 8, 10, and 17. The table also gives the average ratio (O_3/NO_z, etc.) for the data displayed in the figures.

Table 2. O_3-NO_x-VOC Sensitivity and Critical Ratios

	Peak	Peak O_3 With Reduced						
	O_3	VOC	NO_x	$\frac{O_3}{NO_z}$	$\frac{H_2O_2}{NO_z}$	$\frac{H + ROOH}{NO_z}$	$\frac{O_3}{2H_2O_2 + NO_z}$	$\frac{O_3}{2perox + NO_z}$
July 13 at 1400 LT								
J13: standard scenario	135.	124.	119.	7.0	0.12	0.23	5.6	4.8
B1: lower biogenic VOC	118.	102.	103.	7.1	0.12	0.19	5.8	5.1
HC: higher total VOC	150.	144.	125.	7.7	0.16	0.39	5.8	4.3
D5: 5 cm s^{-1} deposition	134.	123.	118.	8.3	0.11	0.24	6.8	5.6
RUC mixing heights	127.	122.	112.	7.9	0.15	0.26	6.1	5.2
RUC and higher VOC	133.	127.	114.	8.3	0.16	0.33	6.2	5.0
Observed	146.			9.3	0.20	0.44	7.0	4.8
July 13 at 1600 LT								
J13: standard scenario	148.	134.	134.	7.2	0.10	0.19	6.0	5.2
B1: lower biogenic VOC	123.	107.	111.	6.9	0.09	0.15	5.9	5.3
HC: higher total VOC	170.	160.	143.	8.0	0.14	0.34	6.3	4.8
D5: 5 cm s^{-1} deposition	147.	132.	133.	8.8	0.09	0.20	7.4	6.2
D5H: high deposition and VOC	160.	148.	138.	9.1	0.11	0.28	7.5	5.8
RUC mixing heights	137.	131.	117.	9.0	0.17	0.31	6.8	5.6
RUC and higher VOC	142.	137.	119.	9.4	0.19	0.40	6.8	5.2
July 11								
J11: standard scenario	119.	107.	106.	8.8	0.11	0.20	7.2	6.3
Observed	132.			9.8	0.18	0.42	7.3	5.0
July 12								
J12: standard scenario	125.	116.	109.	9.0	0.16	0.31	6.8	5.6
July 18								
J18: standard scenario	86.	85.	73.	12.0	0.41	0.39	6.5	5.5
Observed	82.			12.4	0.16	0.34	9.6	7.3

The table shows peak simulated peak O_3 in the Nashville area and the predicted change in peak O_3 resulting from 35% reductions in either anthropogenic VOC or NO_x, along with values of critical ratios concurrent with peak O_3.

Table 3. Distribution of Photochemical Indicator Values for NO_x- and VOC-Sensitive Chemistry

	VOC-Sensitive Locations		NO_x-Sensitive Locations	
Indicator	50th Percentile	95th Percentile	5th Percentile	50th Percentile
O_3/NO_z				
J13: standard	6.6	6.9	8.6	12.5
J13B: low biogenics	6.3	7.3	8.4	12.4
D5B: high deposition	8.8	9.9	10.5	16.8
D1B: low deposition	6.7	7.1	7.6	11.1
Ch: prior chemistry	6.4	7.4	8.1	12.0
J13B at noon	6.24	7.0	6.0	9.3
T: low temperature	5.8	6.7	6.5	9.2
H_2O_2/NO_z				
J13: standard	0.15	0.16	0.20	0.40
J13B: low biogenics	0.13	0.17	0.17	0.31
D5B: high deposition	0.13	0.17	0.18	0.37
D1B: low deposition	0.17	0.21	0.21	0.39
Ch: prior chemistry	0.16	0.19	0.25	0.48
J13B at noon	0.15	0.17	0.14	0.28
T: low temperature	0.07	0.11	0.09	0.18
Total peroxides/NO_z				
J13: standard	0.28	0.30	0.41	0.92
J13B: low biogenics	0.20	0.27	0.29	0.59
D5B: high deposition	0.22	0.30	0.35	0.79
D1B: low deposition	0.25	0.33	0.35	0.70
Ch: prior chemistry	0.24	0.28	0.34	0.80
J13B at noon	0.23	0.26	0.26	0.54
T: low temperature	0.12	0.18	0.18	0.37

The table shows 50th percentile and 95th percentile indicator values (with percentile ordering by indicator value) for VOC-sensitive locations and 5th and 50th percentile indicator values for NO_x-sensitive locations, in each model scenario. VOC-sensitive locations are defined as locations with peak O_3>80 ppb, peak O_3 reduced by at least 5 ppb in simulations with 35% reductions in anthropogenic VOC emissions, and peak O_3 lower by at least 5 ppb in simulations with reduced VOC relative to the equivalent simulation with reduced NO_x. An analogous definition is used for NO_x-sensitive locations.

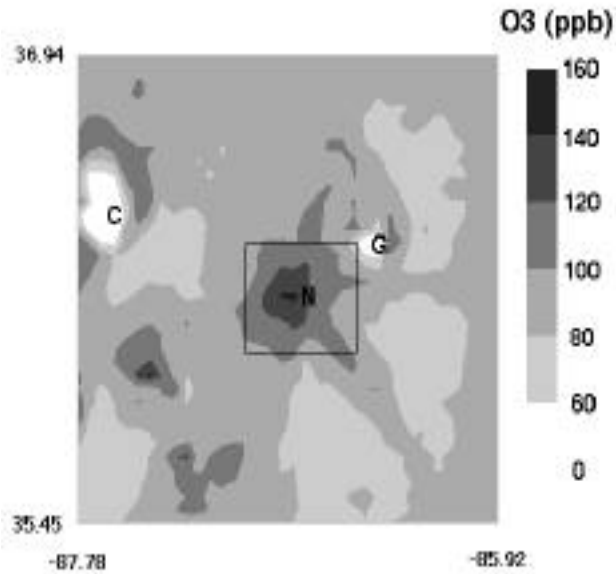

Figure 1. O_3 at 2 pm. July 13 in the standard model scenario for the fine-grid model domain (35.45-36.94 latitude, 85.92-87.78 longitude). The letters N, G and C represent downtown Nashville and the Gallatin and Cumberland power plant plumes. The rectangular lines and diagonal represents the flight path of the G1 aircraft between 1 and 2 pm on July 13.

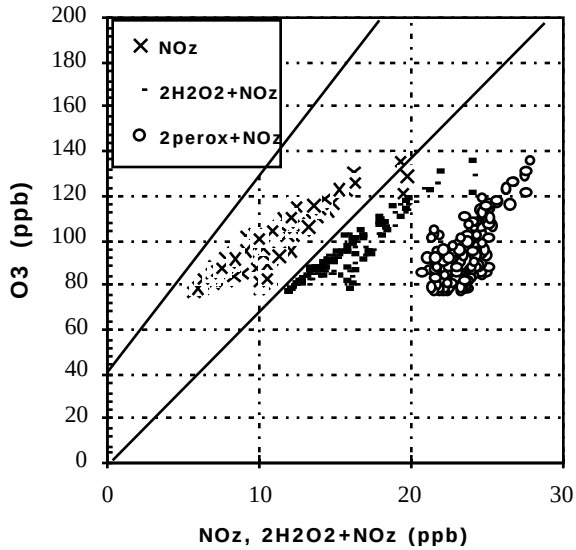

Figure 3. Correlation between O_3 and NO_z (X's), $2H_2O_2$+NO_z (dashes) and 2peroxides+NO_z (circles), all in ppb, in the standard model scenario at 2 pm, July 13. The lines give reference values for (i) a slope of 9:1 and y-intercept 40 ppb, and (ii) a slope of 7:1 and y-intercept zero.

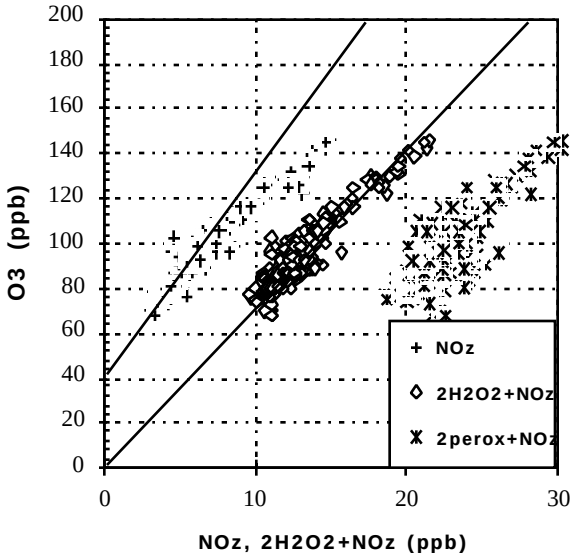

Figure 2. Correlation between O_3 and NO_z (crosses), $2H_2O_2$+NO_z (diamonds) and 2peroxides+NO_z (asterisks), all in ppb, from measurements aboard the G1 aircraft between 1 and 2 pm, July 13. The lines give reference values for (i) a slope of 9:1 and y-intercept 40 ppb, and (ii) a slope of 7:1 and y-intercept zero.

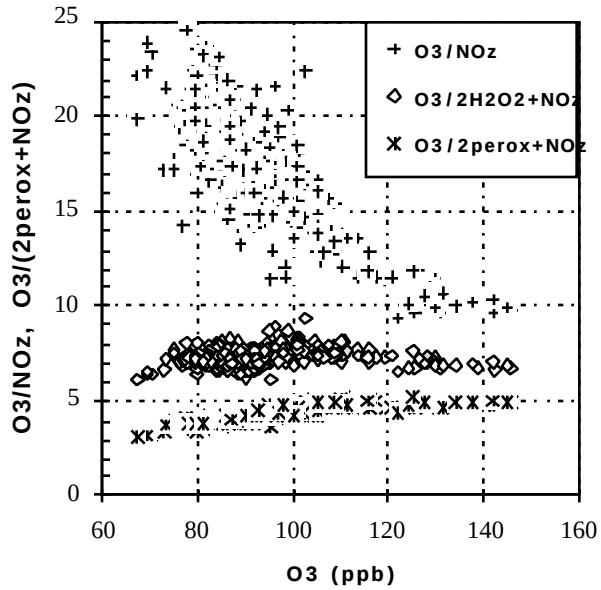

Figure 4. The ratios O_3/NO_z (crosses), $O_3/(2H_2O_2+NO_z)$ (diamonds) and O_3/(2peroxides+NO_z) (asterisks), plotted vs. O_3 in ppb, from measurements aboard the G1 aircraft between 1 and 2 pm, July 13.

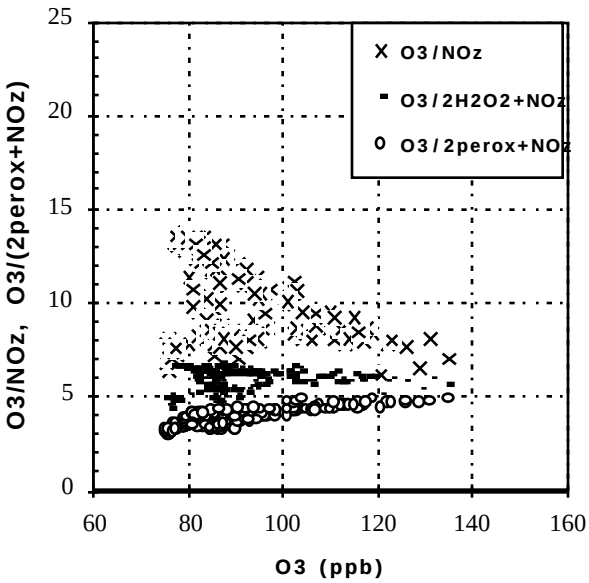

Figure 5. The ratios O_3/NO_z (X's), $O_3/(2H_2O_2+NO_z)$ (dashes) and O_3/(2peroxides+NO_z) (circles), plotted vs. O_3 in ppb, in the standard model scenario at 2 pm, July 13.

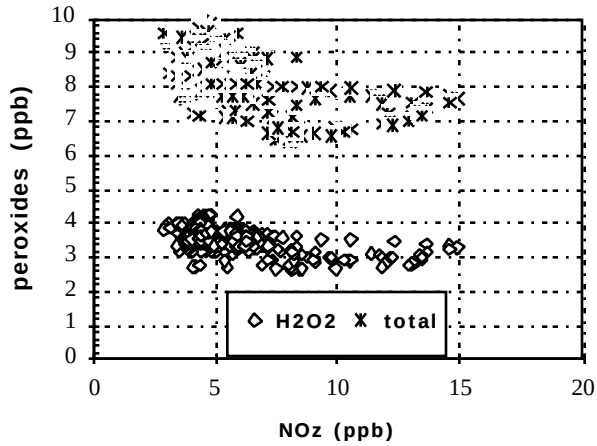

Figure 7. Correlation between NO_z and H_2O_2 (diamonds) and between NO_z and total peroxides (asterisks), all in ppb, from measurements aboard the G1 aircraft between 1 and 2 pm, July 13.

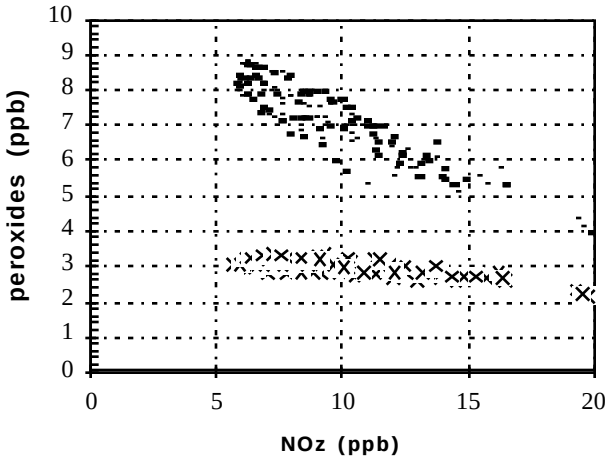

Figure 6. Correlation between NO_z and H_2O_2 (X's) and between NO_z and total peroxides (dashes), all in ppb, in the standard model scenario at 2 pm, July 13.

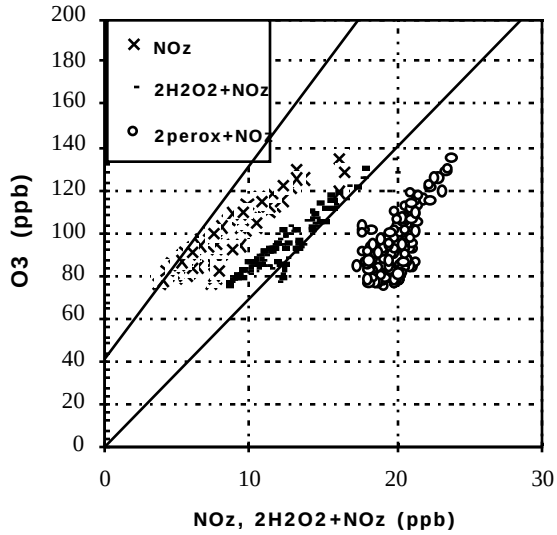

Figure 8. Correlation between O_3 and NO_z (X's), $2H_2O_2+NO_z$ (dashes) and 2peroxides+NO_z (circles), all in ppb, in the model scenario with high dry deposition (5 cm s^{-1}) at 2 pm, July 13.

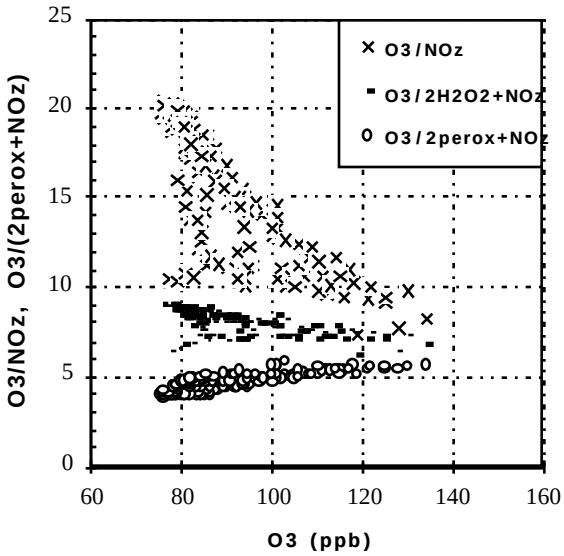

Figure 9. The ratios O_3/NO_z (X's), $O_3/2H_2O_2+NO_z$ (dashes) and O_3/2peroxides+NO_z (circles), plotted vs. O_3 in ppb, in the model scenario with high dry deposition (5 cm s^{-1}) at 2 pm, July 13.

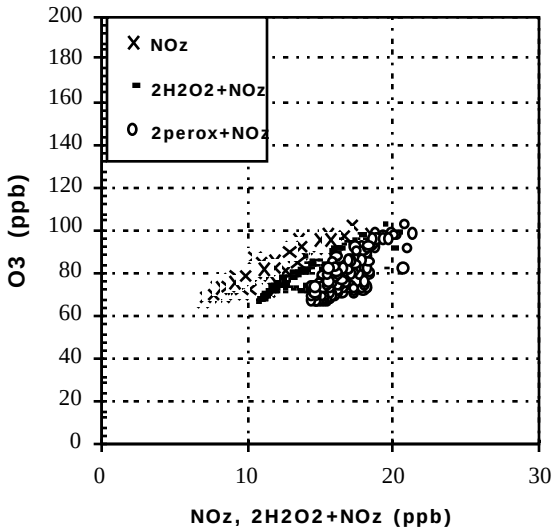

Figure 10. Correlation between O_3 and NO_z (X's), $2H_2O_2+NO_z$ (dashes) and 2peroxides+NO_z (circles), all in ppb, in the model scenario with temperatures reduced by 10 K at 2 pm, July 13.

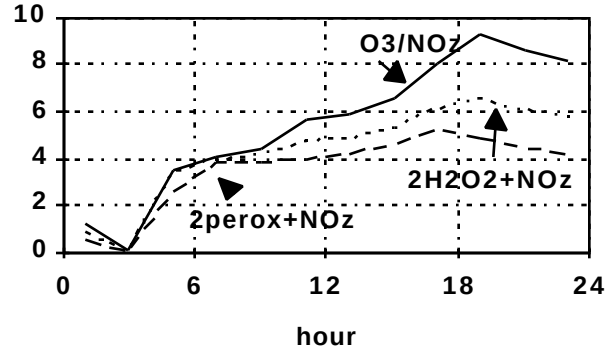

(a)

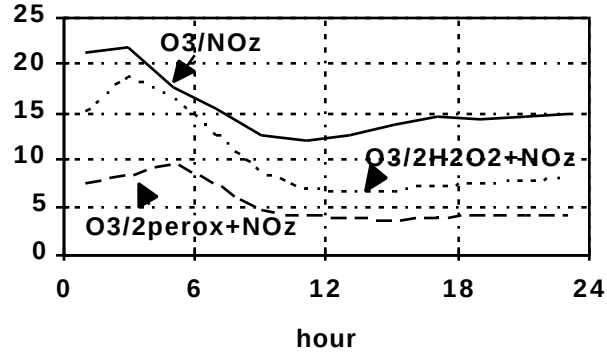

(b)

Figure 11. Diurnal variation in O_3/NO_z (solid line), $O_3/(2H_2O_2+NO_z)$(short dashes) and O_3/(2peroxides+NO_z) (long dashes) at (a) downtown Nashville and (b) a rural site 75 km southeast of Nashville in the standard model scenario for July 13. Hour represents local standard time.

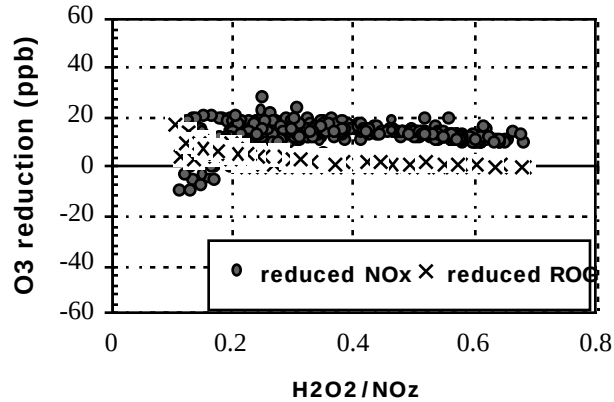

Figure 12. Reduction in O_3 at 4 pm, July 13, resulting from either a 35% decrease in anthropogenic VOC emissions (X's) or a 35% reduction in NO_x emissions (solid circles) at each location in the urban model domain, plotted against H_2O_2/NO_z at 4 pm at the same location as the predicted reduction. Results are based on the standard model scenario.

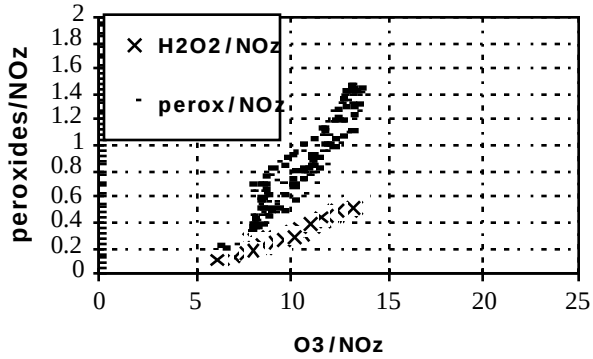

(a)

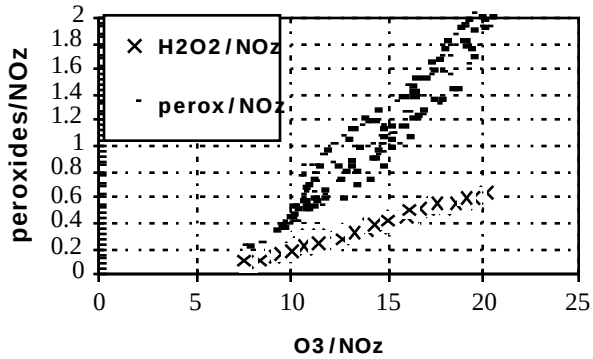

(b)

Figure 13. H_2O_2/NO_Z (X's) and peroxides/NO_Z (dashes) vs. O_3/NO_Z at 2 pm, July 13 in (a) the standard model scenario and (b) the scenario with increased dry deposition (D5).

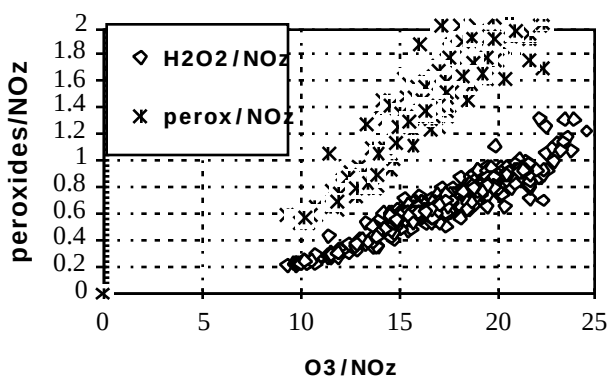

Figure 14. H_2O_2/NO_Z (circles) and peroxides/NO_Z (asterisks) vs. O_3/NO_Z from measurements aboard the G1 aircraft between 1 and 2 pm, July 13.

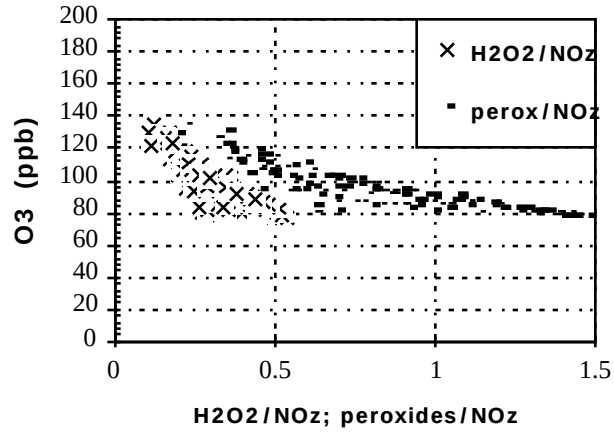

Figure 15. O_3 vs. H_2O_2/NO_Z (X's) and O_3 vs. peroxides/NO_Z (dashes), all in ppb, in the standard model scenario at 2 pm, July 13.

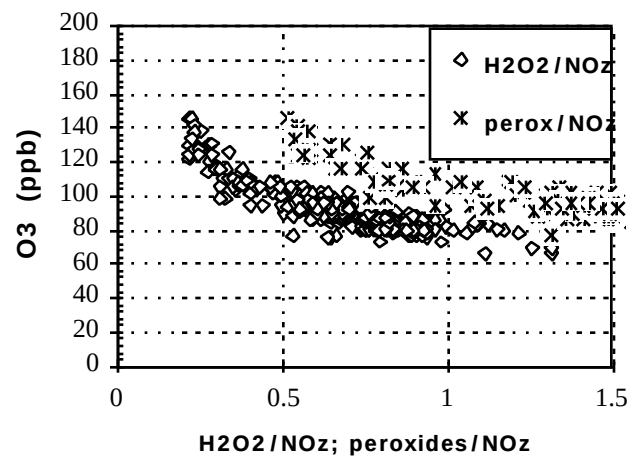

Figure 16. O_3 vs. H_2O_2/NO_Z (diamonds) and O_3 vs. peroxides/NO_Z (asterisks), all in ppb, from measurements aboard the G1 aircraft between 1 and 2 pm, July 13.

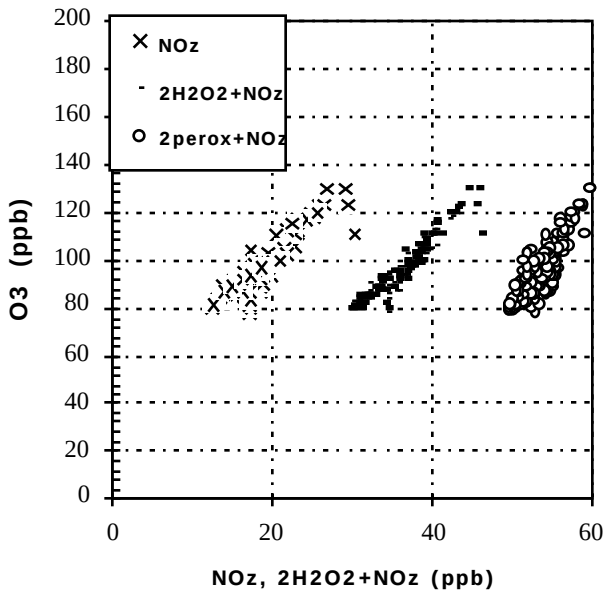

Figure 17. Correlation between O_3 and NO_z (X's), $2H_2O_2$+NO_z (dashes) and 2peroxides+NO_z (circles), all in ppb, from the standard scenario with zero deposition and photochemical losses for NO_z and peroxides at 2 pm, July 13.